land

MDPI

Article

Quantification and Flow Simulation of Ecosystem Service Supply and Demand in the Yellow River Delta High-Efficiency Eco-Economic Zone

Wenjun Liu [1], Xiangyi Ma [1], Qian Sun [2], Wei Qi [1,*] and Xinyang Yu [1,3,*]

[1] College of Resources and Environment, Shandong Agricultural University, Taian 271018, China
[2] College of Information Science and Engineering, Shandong Agricultural University, Taian 271018, China
[3] Institute of Geographic Sciences and Natural Resources Research, Chinese Academy of Sciences, Beijing 100101, China
* Correspondence: qiwei@sdau.edu.cn (W.Q.); yuxy.12b@igsnrr.ac.cn (X.Y.)

Abstract: The identification of supply and demand areas for ecosystem services (ES) and the simulation of ES flows are essential for optimizing ESs to achieve socio-economic sustainable development. However, the selection of investigation methods and simulation model remains a persistent challenge. This study selected the Yellow River Delta High-Efficiency Eco-Economic Zone in China as the case study area and assessed the habitat quality and carbon sequestration services for 2000, 2010, and 2020. The quantile regression method was employed to quantify the impacts of land use structure on balancing the supply and demand of ESs. The minimum cumulative resistance model, circuit corridor model, and wind direction model were utilized to analyze changes in flux and flow direction of ESs' supply and demand. The results demonstrated that the following: (1) the supply of ESs generally increased, with a significant rise in demand for carbon sequestration service and a declining trend in habitat quality service demand. (2) A clear spatial mismatch existed between the supply and demand of ESs. (3) The impact of land use structure on the balance of ES supply and demand is complex. (4) Habitat quality and carbon sequestration services exhibited distinct spatial clustering patterns. (5) The flow patterns of habitat quality service were characterized by specific supply and demand areas, with corridors and pinch points indicating the flow paths and potential barriers; not all demand areas for carbon sequestration service can be satisfied due to variations in service levels and geographical distance. The innovation of this study lies in the following aspects: (1) it acknowledges the uniqueness of ecosystem services, with a focus on assessing habitat quality and carbon sequestration services; (2) it precisely quantifies the flow of ecosystem services, analyzes the spatial dynamics of service flows, and investigates the impact of changes in land-use structure on these flows; (3) it strengthens the correlation between the supply and demand of ecosystem services and socio-economic activities, uncovers the contradictions between supply and demand along with their underlying causes, and proposes effective strategies for resolution. The findings can provide theoretical and methodological references for the optimization of ES.

Keywords: ES flow; quantile regression; InVEST model; linkage mapper; breakpoint modeling

check for updates

Citation: Liu, W.; Ma, X.; Sun, Q.; Qi, W.; Yu, X. Quantification and Flow Simulation of Ecosystem Service Supply and Demand in the Yellow River Delta High-Efficiency Eco-Economic Zone. *Land* **2024**, *13*, 1784. https://doi.org/10.3390/land13111784

Academic Editors: Lindsay Claire Maskell and Claire Wood

Received: 20 September 2024
Revised: 18 October 2024
Accepted: 24 October 2024
Published: 30 October 2024

Copyright: © 2024 by the authors. Licensee MDPI, Basel, Switzerland. This article is an open access article distributed under the terms and conditions of the Creative Commons Attribution (CC BY) license (https://creativecommons.org/licenses/by/4.0/).

1. Introduction

Ecosystem service (ES) flow, as a derived concept of ES, is the spatial displacement of services between the place where they are generated and the place where they are used or the transfer between providers and consumers [1–4]. The investigation of ecosystem services flow holds significant importance in the development of policies for ecological sustainability, planning for ecological restoration and protected areas, as well as designing patterns for ecological security and networks [5].

Exploring the supply and demand of ES is a crucial part of ES flow research. Currently, methods for spatializing the supply and demand of ESs include land use estimation [6], ecological process simulation [7], spatial overlaying of data [8], expert empirical discrimination [9], the ARIES method (Artificial Intelligence for ESs) [10], and the InVEST model (Integrated Valuation of ESs and Trade-offs) [11]. However, after spatial mapping of ESs and demand, it was found that spatial mismatches between hotspots of ES supply and demand can lead to a flow of services from areas of oversupply to areas of undersupply [12]. In this context, the study of ES flow has received attention, and related research has become an international hotspot. Understanding the conceptual connotation of ES flows and clarifying their quantification methods are the basic prerequisites for promoting the effective practice of ES flows [13]. Li et al. (2022) introduced the concepts, quantification methods, and application cases of ES flows, and proposed future research directions for ES flows [14]. Zhang et al. (2023) analyzed the flow of ESs within a watershed and between a watershed and an external region in a meta-coupling framework [15]. Wang et al. (2023) identified the relationship between four socio-ecological processes (product transfer, material cycling, energy flow, and information transfer) and the spatial flow of ESs, and based on this, provided an overview of methods for quantifying spatial flows in ecosystems [16]. Du et al. divided the region into ecological output and ecological input zones based on ES supply and demand. The breaking point model and field model were introduced to reveal the characteristics of ES flows from output to input zones, and an ecological compensation policy for the study area was formulated based on the ES supply and demand model [17]. Jiang et al. (2021) quantified the pattern of ES supply and demand by using the ES matrix approach and explored the factors affecting the balance between ES supply and demand using spatial econometric modeling and geographically weighted regression methods [18]. At present, by quantifying the supply and demand of ESs, analyzing the temporal and spatial patterns of change in the supply and demand patterns based on the regional supply and demand balance relationship, and then determining the flow path of ESs has become the mainstream paradigm of ES flow research [19]. Nonetheless, the majority of current research has centered on delineating the zones of supply and compensation for ecosystem service flows by examining disparities in ES supply and demand, frequently overlooking the distinct characteristics of various ecosystem services. Case in point, Xiong et al. (2023) identified 10 types of ecosystem services, formulated an exhaustive model for ecosystem service supply and demand, and evaluated the expanse and magnitude of the collective ecosystem service flows through the incorporation of a breakpoint model alongside a field strength model [20]. Wu et al. (2024) employed the fracture point model to mimic the flow dynamics of carbon sequestration services in Tibet, subsequently devising a tiered eco-compensation strategy in response [21]. Lin et al. (2024) investigated the flow trajectories of water-provisioning services from the supply to the demand zones within a watershed, and in conjunction with the effects of land-use changes on these services, proposed a tailored eco-compensation plan [22]. Su et al. (2024) examined the fluctuations in ecosystem service (ES) supply and demand at the urban level across China from 2010 to 2020. They delved into the natural and social determinants influencing the shifting patterns of ES supply and demand [23]. The intricate processes of material exchange and energy movement within and beyond ecosystem services are profoundly complex. The orientations of these service flows exhibit a rich diversity, ranging from unidirectional transmission to circular movement and encompassing feedback mechanisms. This complexity introduces substantial challenges in precisely quantifying the flow trajectories when attempting to analyze a variety of ecosystem services with distinct characteristics in a unified framework, thereby constraining the practical application of the research findings. Hence, future scholarship must delve deeper into the flow characteristics of diverse ecosystem services with greater specificity and focus. It is imperative to conduct a comprehensive examination of the entire ecosystem services (ES)

lifecycle, encompassing generation, flow, and utilization. Such an approach is essential for enhancing the practical utility and strategic guidance of research outcomes.

The Yellow River Delta High-Efficiency Eco-Economic Zone is situated in the eastern coastal region of China and plays a pivotal role as both a national strategy and an integral component of the regional coordinated development strategy. It serves as a vital ecological protection barrier for the Yellow River while simultaneously functioning as an indispensable economic hub that facilitates sustainable development in China [24]. The region has outstanding advantages in land resources, with natural resources such as wetlands, oil, natural gas, and brine, and is one of the most typical estuarine wetlands in the warm-temperate zone. Evaluating the regional ESs, including habitat quality and climate regulation, is pivotal for comprehending and augmenting the overall worth of the regional ecosystem. This assessment aids in preserving the ecological equilibrium both regionally and for the nation at large. The region itself serves as a critical benchmark for ecological preservation efforts in other river deltas across the globe. It promotes comparative research on ecological service functions across different regions, furthering global initiatives on climate change adaptation and biodiversity conservation. Moreover, it yields valuable insights into ecosystem management and restoration practices, fostering international dialogue and collaboration on sustainable development strategies. It provides a robust scientific foundation for the formulation and governance of global environmental policies. Additionally, it stands as a significant reference point for forecasting future trends in global ecological and environmental transformations. The development experience of the Yellow River Delta High-Efficiency Eco-Economic Zone has provided references for other regions around the globe and has become one of the most exemplary regions in the world. However, the acceleration of urbanization in recent years has exerted considerable pressure on local ecosystems, and regional ecosystems are facing great challenges [25], with the ecosystems' carbon storage capacity continuing to weaken, and the coastal zone ecosystems being degraded to varying degrees [26]. In-depth studies are urgently needed to analyze the spatial flow patterns of ES functions, clarify the transmission paths between supply and demand areas, and explore the impact of land-use patterns on the relationship between supply and demand for ESs.

This study thus focused on the Yellow River Delta High-Efficiency Eco-Economic Zone and selected habitat quality and carbon sequestration services for assessment and analysis, considering the unique ecological conditions and ecological resources of the study area. The objective is to quantify and spatially identify the supply and demand of ESs in the three periods of 2000, 2010, and 2020 using multi-models, analyze the impact of land use patterns on the ratio of ES supply and demand, and analyze changes in flow direction and fluxes of ES supply and demand using the circuit corridors and wind direction methods. The study aims to provide actionable insights for the ecological restoration of the Yellow River Delta High-Efficiency Eco-Economic Zone while optimizing its pattern of ecological service supply and demand to foster sustainable socio-economic development.

2. Study Area and Data Source

2.1. Study Area

The Yellow River Delta High-Efficiency Eco-Economic Zone (36°25′27″–38°16′17″ N, 116°56′14″–120°18′15″ E) is located in the estuaryof China's mother River–Yellow River [27]. The regional scope includes the whole area of Dongying and Binzhou cities and parts of Weifang, Zibo, Yantai, and Dezhou cities, covering a total area of 26,500 km^2 (Figure 1). The study area has a warm temperate continental monsoon climate, with four distinct seasons, hot and humid summers, cold and dry winters. The average annual temperature is 12.8 °C, and the average annual precipitation ranges from 530 to 630 mm. The topography was dominated by plains, high in the south and low in the north. The study area is located in the intertwined zone of multiple ecosystems, with resources such as river and sea confluence,

coastal beach landscape, oil, gas, and minerals, which is the area with the most potential for development in China, and is a special ecological function area and a typical ecologically sensitive area [28].

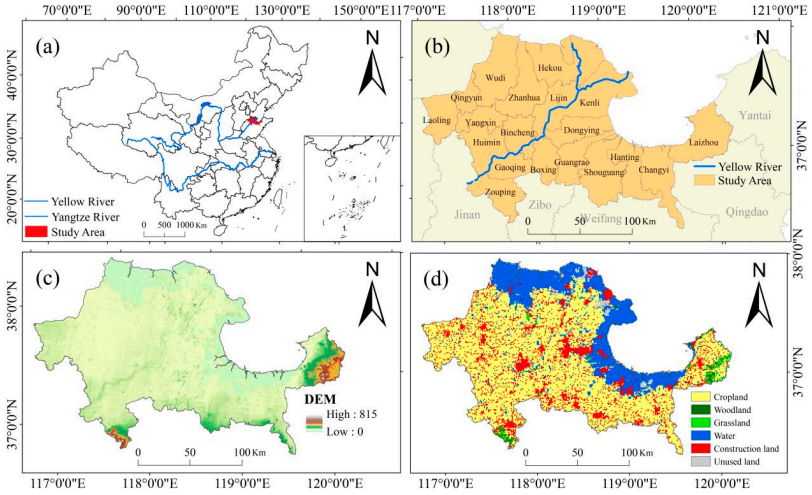


Figure 1. Location of the case study area. (**a**) The case study area in China; (**b**) administrative division of the study area; (**c**) DEM of the study area; (**d**) land-use pattern of the study area.

2.2. Data Source

Data used in this study include land use data, digital elevation model (DEM), Normalized Different Vegetation Index (NDVI), population density data, per capita GDP data, as well as vector data of road network, river, weather station, etc. The data sources are listed in Table 1, and were unified in the projected coordinate system (Albers_Conic_Equal_Area) and spatial resolution (1 km).

Table 1. Data sources used in this study.

Data Name	Data Type	Data Sources
Land use data	Raster data	Environmental Science and Data Center (https://www.resdc.cn, accessed on 3 April 2024)
DEM	Raster data	Geospatial Data Cloud (https://www.gscloud.cn, accessed on 3 April 2024)
NDVI	Raster data	Global Resources Data Cloud (http://www.gis5g.com, accessed on 3 April 2024)
Population density data	Raster data	World Pop (https://hub.worldpop.org, accessed on 3 April 2024)
Per capita GDP data	Raster data	Resource and Environmental Science Data Platform (https://www.resdc.cn, accessed on 3 April 2024)
Traffic road data	Vector data	GEOVIS Earth Open Platform (https://open.geovisearth.com, accessed on 3 April 2024)
River system data	Vector data	Global Resources Data Cloud (http://www.gis5g.com, accessed on 3 April 2024)
Meteorological data	Vector data	National Climatic Data Center (ftp://ftp.ncdc.noaa.gov/pub/data/noaa/isd-lite/, accessed on 3 April 2024)

3. Methods

The workflow of this study is shown in Figure 2.

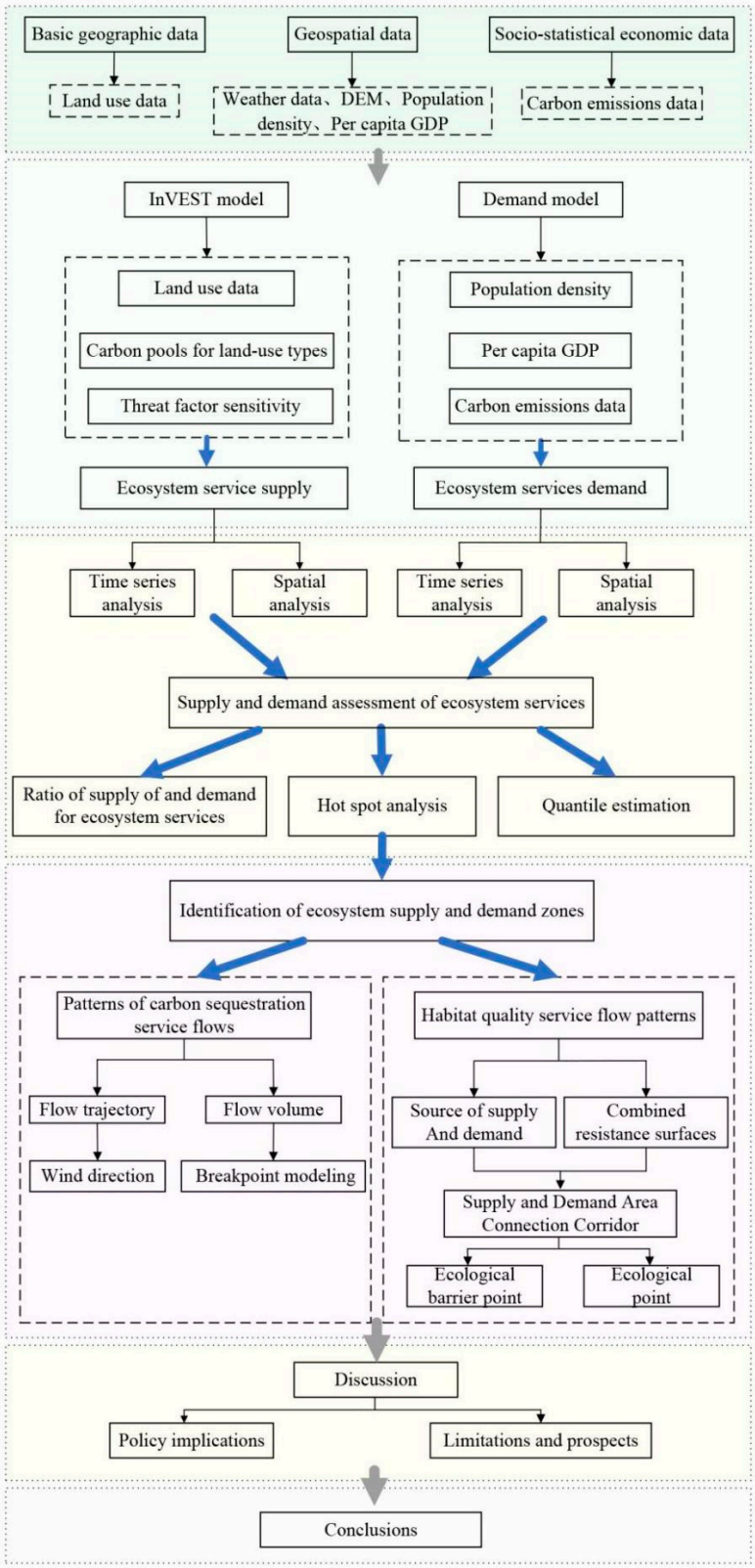


Figure 2. Study workflow.

3.1. ESs Quantification

The InVEST model was utilized to quantify the HQ and CS within the research region for years of 2000, 2010, and 2020. Additionally, it facilitated an assessment of the spatial

and temporal distribution characteristics of ESs as well as the evolving patterns of such services in the study area.

3.1.1. Assessment of Supply and Demand Capacity for HQ

HQ

$$Q_{ij} = H_j\left[1 - \frac{D_{ij}^z}{\left(D_{ij}^z + k^z\right)}\right] \quad (1)$$

where Q_{ij} and D_{ij}^z are the HQ and the degree of habitat degradation of grid i in land use type j, respectively; H_j is the habitat suitability for land use type j; z is the normalization index, the default constant of the model, which takes the value of 2.5; k is the half-saturation constant, which takes the value of 0.5 [29,30].

HQ Demand

The degree of land development, population density, and per capita GDP are selected as indicators reflecting regional demand for ESs dominated by human activities [31].

$$\begin{aligned} D_i &= a_{i1} \times \log_{10}(a_{i2}) \times \log_{10}(a_{i3}) \\ D_{HQi} &= \frac{D_i - D_{imin}}{D_{imax} - D_{imin}} \end{aligned} \quad (2)$$

where D_i is the HQ demand of grid i and a_{i1} is the land use development intensity of grid i, i.e., the area of built-up land as a percentage of the total land area of the region; a_{i2} is the population of grid i (people/km^2), which reflects the human demand for habitat quality; a_{i3} is the GDP value of grid i (million yuan/km^2). D_{HQi} is the HQ demand of grid i after normalization, D_{imax} and D_{imin} are the maximum and minimum values of the HQ requirements in all grids, respectively.

3.1.2. Quantification of Supply and Demand Capacity for CS

CS Supply

The yearly carbon sequestration is estimated by the type of land use and the carbon density of each type of land use, and the calculation formula is as follows:

$$C_{total} = C_{above} + C_{below} + C_{soil} + C_{dead} \quad (3)$$

where C_{total} is the total carbon stock in the study area (t); C_{above} is the aboveground biogenic carbon (t); C_{below} is the belowground biogenic carbon (t); C_{soil} is the soil carbon (t); and C_{dead} is the dead organic carbon (t). Carbon density reflects the quantity of carbon sequestered per unit area across various land types. The values for carbon density associated with different land uses were ascertained about analogous study regions [30].

CS Demand

1. Demand of CS

The calculation of CS demand adopts the population density method [32], which takes the carbon emissions of the research region as the total demand, and spatializes the demand through population density and per capita carbon emissions, and the calculation formula is as follows:

$$C = C_p \times P_{\rho o \rho} C_p = \frac{C_c}{n} = \frac{C_z + C_j}{n} \quad (4)$$

where C is the total demand for CS (t); C_p is the per capita carbon emission (t/person); $P_{\rho o \rho}$ is the population density (person/km^2), n which is the total population of the study area; C_c is the total carbon emission (t), and C_z and C_j are the direct carbon emission and indirect carbon emission (t), respectively.

2. Quantification of carbon emission accounting

The direct carbon emission coefficient method is utilized to account for the carbon emissions from cropland, woodland, grassland, watersheds, unused land, and the calculation formula is:

$$C_z = \sum e_i = \sum s_i \times a_i \tag{5}$$

where C_z is the direct carbon emissions (t); e_i is the carbon emissions from the land-use type; s_i is the area of the land-use type i; and a_i is the carbon emission factor of the land-use type i. Indirect carbon emissions are calculated by using the IPCC inventory method to account for the carbon emissions caused by energy consumption in people's production activities, converting the different types of energy consumed, such as oil, coal, and electricity, into standard coal, and then multiplying them by their respective energy carbon emission coefficients and finally summing them up to estimate the total carbon emissions of the construction land use land type.

Sixteen types of energy consumption types, including raw coal, washed coal, other washed coal, LPG, crude oil, gasoline, kerosene, diesel, fuel oil, coke, natural gas, liquefied natural gas, coke oven gas, blast furnace gas, dry gas from the refinery, and other gas, were selected as the study indicators. The carbon emissions in the research region were calculated indirectly by calculating the carbon emissions from construction land in Shandong Province with the following formula [33].

$$C_s = \sum a_i \times \theta_i \times \varphi_i C_j = C_s \times \frac{a}{A} \tag{6}$$

where C_s is the indirect carbon emissions of Shandong province; a_i is the consumption of energy i in Shandong province; θ_i is the standard coal conversion factor of energy i; φ_i is the carbon emission factor of energy i. C_j is the indirect carbon emissions of the study area (t); A is the area of construction land in Shandong province (km^2); a is the area of construction land in the research region (km^2).

3.2. Assessment of ES Supply and Demand

3.2.1. Supply–Demand Ratio Model of ES

ES supply–demand ratio (ESDR model) was used to explore the supply–demand relationship between habitat quality and carbon sequestration services in the research region [34], and the calculation formula was as follows:

$$ESDR = \frac{S - D}{(S_{max} + D_{max})/2} \tag{7}$$

where $ESDR$ is the ESs supply–demand ratio, S is the supply of a service, D is the demand for a service, S_{max} is the maximum supply of a service, and D_{max} is the maximum demand for a service. When $ESDR > 0$, ESs are in surplus; when $ESDR = 0$, ecosystem supply and demand are in balance; when $ESDR < 0$, ecosystems are in deficit.

3.2.2. Quantile Regression Analysis

The quantile regression model was established to analyze the impact of each type of land use on the balance of ES supply and demand, with the index of ES supply–demand ratio as the explanatory variable and the proportion of each type of land use as covariates [35,36]. The formula is as follows:

$$Q_\theta(Y|X) = X'\beta(\theta) \tag{8}$$

where $Q_\theta(Y|X)$ is the value of the X explanatory variable Y at the θ quantile when the explanatory variable X is explicit. Among them, the explanatory variables are the proportion of cropland, the proportion of woodland, the proportion of grassland, the proportion of watershed, the proportion of construction land, and the proportion

of unused land. $\beta(\theta)$ denotes the vector of regression coefficients at the θ quantile, satisfying the following conditions:

$$\beta_\theta = min\left\{ \sum_{i:Y \geq X'} \theta|yY - X'\beta| + \sum_{i:Y < X'\beta(\theta)} \theta|(1-\theta)|Y - X'\beta(\theta)| \right\} \quad (9)$$

When θ takes the value of 0~1, it can describe all the conditional distribution trajectories of Y on X. In this study, we set 0.1, 0.3, 0.5, 0.7, and 0.9 quantile parameter estimation results to analyze the role of different land use types on different ES supply and demand balance indices.

3.2.3. Hotspot Analysis

To clarify the spatial distribution characteristics of ES supply and demand zones in the research region, the ES supply and demand ratio (ESDR) of the study area was processed by using hot spot analysis [37]. The formula is as follows:

$$G_i^* = \frac{\sum_{i=1}^{n} w_{ij}x_i - \overline{X}\sum_{i=1}^{n} w_{ij}}{\left[\sqrt{\frac{\sum_{i=1}^{n} x_i^2}{n-1} - \left(\overline{X}\right)^2}\right]\sqrt{\frac{n\sum_{i=1}^{n} w_{ij}^2 - \left(\sum_{i=1}^{n} w_{ij}\right)^2}{n-1}}} \quad (10)$$
$$\overline{X} = \frac{\sum_{n=1}^{n} x_i}{n}$$

where x_i is the supply–demand ratio of an ES for grid i; w_{ij} is the spatial weight matrix between grid i and grid j; $\overline{X}$ is the average value of the supply–demand ratio for a given ES; and n is the total number of patches. In this study, the supply–demand ratio (ESDR) of HQ and CS in the study area was assigned at the township (sub-district) scale using spatial statistical tools (ArcGIS 10.8), and the study was carried out through the hotspot analysis (Getis-Ord Gi*) in the spatial statistical tools.

3.3. Quantification of ES Flow

3.3.1. Habitat Quality Service

The minimum cumulative resistance model considers the product of the distance traveled by a species from its source to its destination through different resistance units and the value of the landscape resistance traversed to be the "cost" of migration, and the corridor with the lowest cumulative cost is the optimal corridor [38]. The flow of electrical current is analogous to the processes underlying habitat quality service flows, where the intensity and direction of the currents serve as a proxy for the magnitude and direction of species migration and gene flow within ecological systems. This method predicts species migration paths and fluxes between different landscape units without considering actual species movement [39]. The calculation formula is as follows:

$$I = \frac{V}{R_{eff}} \quad (11)$$

where I is the current through the conductor; V is the voltage across the conductor; and R_{eff} is the effective resistance of the conductor, used to reflect the degree of spatial isolation of the node indicators. In a parallel circuit with multiple branches and constant resistance in each branch, R_{eff} decreases with increasing number of branches; R_{eff} is an indicator of the degree of spatial isolation between nodes.

3.3.2. Carbon Sequestration Service

Wind action contributes to the transport and distribution of atmospheric carbon dioxide and other carbon compounds in ecosystems, which in turn affects carbon sequestration in vegetation and carbon storage processes in soils. Wind data are usually variable, and in this study, the maximum frequency wind direction was selected to characterize the general

trend of wind direction in the area over a specific time period based on the meteorological station data of the study area in 2020.o simulate the flow path of carbon sequestration service, this study employed the inverse distance weighting interpolation tool for wind direction data analysis [40]. The calculation formula is as follows:

$$Z(S_0) = \sum_{i=1}^{N} \lambda_i Z(S_i) \tag{12}$$

where $Z(S_0)$ is the interpolated predicted value at S_0, N is the data of the sample points around the predicted point to be used in the calculation process, λ_i is the weight of each sample point used in the calculation process, and $Z(S_i)$ is the true value obtained at S_i.

The radial distance of CS from the supply area to the demand area is quantified using the breakpoint formula:

$$d_{ij} = \frac{D_{ij}}{1 + \sqrt{N_j / N_i}} \tag{13}$$

where d_{ij} is the radial distance from supply zone i to demand zone j, i.e., the flow radius; D_{ij} is the distance from the core point of supply area i to the core point of demand area j, N_i and N_j are the difference between the supply and demand of ESs in supply area i and demand area j, respectively. If the difference between supply and demand for ESs in demand area j is less than zero, then $d_{ij} = D_{ij}$.

Based on the derived breakpoint distance, the spatial analysis method was utilized to generate a buffer zone with the core of supply area i as the starting point and the breakpoint distance as the radius, and the buffer zone was superimposed on the demand area j. The intersecting portion was the flow area of ESs from supply area i to demand area j. The field model is used to calculate the radiated field strength at the furthest distance from the supply area and is taken to be the average radiation value using the following formula:

$$F_{ij} = \frac{N_i}{d_{ij}^2} \tag{14}$$

The flow of ESs for carbon sequestration services is obtained based on the average radiation value and the area of influence of the supply area on the demand area and is calculated as follows:

$$E_{ij} = F_{ij} \times S_{ij} \times \beta \tag{15}$$

where E_{ij} is the flow of ESs from supply area i to demand area j, S_{ij} is the area of influence of supply area i on demand area j, i.e., the intersection area between the radiation range of supply area i and demand area j. β is the spatial conversion coefficient, whose value ranges from 0 to 1. Referring to the previous study [21], β in this study was set as the value of 0.4.

4. Results

4.1. Spatiotemporal Change

4.1.1. Spatiotemporal Change of ESs

The mean HQ indices for the three years were 0.35, 0.34, and 0.41 (Figure 3), respectively. The high HQs were located in the northern and northeastern coastal areas of the research region, these areas were rich in valuable wetlands, woodland and serve as important habitats for avian and wetland wildlife; low habitat quality regions were found in urban construction areas, which were subject to significant human disturbance. From the temporal perspective, the habitat quality exhibited a downward trend from 2000 to 2010. From 2010 to 2020, the habitat quality experienced a substantial increase with an increase of 20.6%. Over the past two decades, the regions with significantly improved HQs were found in coastal wetlands.

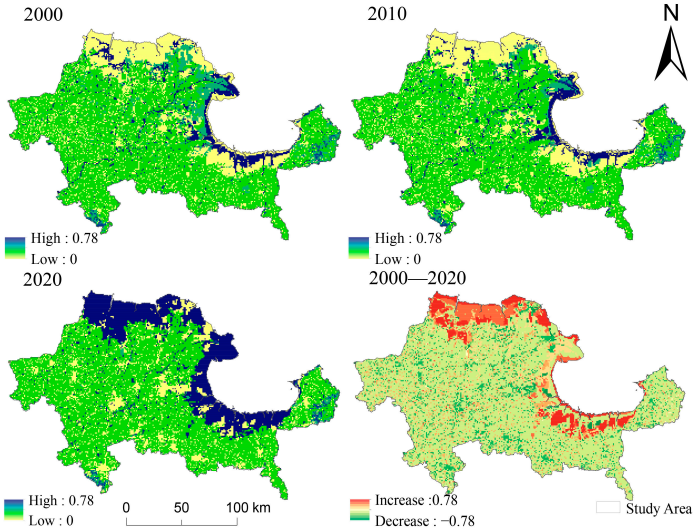


Figure 3. Spatial distribution of HQ.

The carbon storage for 2000, 2010, and 2020 were 8.22 × 10^7, 8.13 × 10^7, and 8.41 × 10^7 tons, respectively (Figure 4). The carbon storage presented a pattern of being lower in the north and higher in the south, decreasing from west to east and from south to north. High-value regions were located in the eastern and southern parts of the research region, where there is a significant proportion of cropland, woodlands, and grasslands. Due to the lower carbon density in water bodies, the low-value regions of carbon storage were found in the northern and northeastern coastal areas, as well as in urban construction land with more frequent human activity. Over the temporal dimension, from 2000 to 2010, the carbon storage exhibited a declining trend. Conversely, from 2010 to 2020, the carbon storage experienced a substantial increase. This upswing was attributed to the advancements made in ecological and environmental protection efforts initiated by the government. The carbon storage increased by 2.80 × 10^6 tons, and the area of low-value regions was substantially reduced. Over the past two decades, the regions with significantly increased carbon storage were found in coastal wetlands. Conversely, the regions with significantly decreased carbon storage were located in urban construction areas, which have been subject to intense human activity interference.

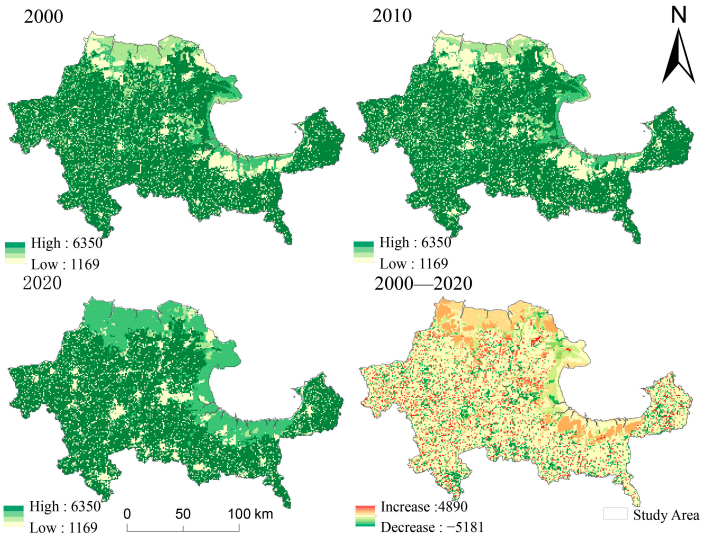


Figure 4. Spatial distribution of CS.

4.1.2. Spatiotemporal Changes of ES Demand

The demand for habitat quality was calculated using socio-economic indicators; these demand values were then treated to be dimensionless and normalized to obtain the habitat quality demand for the study area across the three periods of 2000, 2010, and 2020 (Figure 5). The respective means were 0.53, 0.60, and 0.40. The demand for habitat quality exhibited a trend of initially rising and then decreasing. From a spatial distribution perspective, the overall demand for habitat quality showed a pattern of higher in the south and lower in the north, decreasing progressively from south to north. The regions with high demand for habitat quality were located in the central and southern parts of the study area. Low-value regions were found in the northern parts of the study area. Over the temporal dimension, the demand for habitat quality showed a trend of initial increase followed by a decline. Between 2000 and 2010, with the growth in population and socio-economic development, the demand for habitat quality rose. However, from 2010 to 2020, as the government actively engaged in ecological and environmental protection, a portion of construction land in the northern part of the study area was converted into water bodies, leading to a decrease in land use intensity. This change mitigated the disturbance of human activities on the ecosystem, resulting in a decline in the demand for HQ during this period.

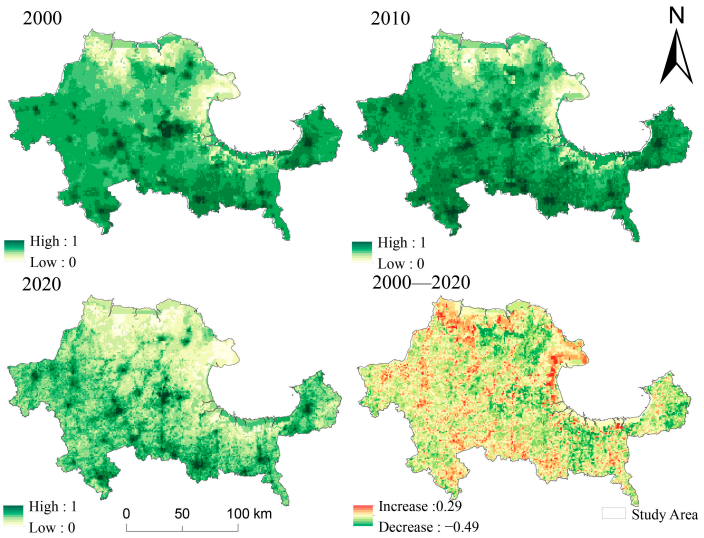


Figure 5. HQ demand and change.

The demand for CS for 2000, 2010, and 2020 was calculated based on per capita carbon emissions and population density, resulting in respective values of 1.48×10^7 tons, 3.92×10^7 tons, and 6.41×10^7 tons. The total demand for carbon sequestration services showed a continuous upward trend. Carbon sequestration demand was jointly determined by per capita carbon emissions and population density, with the spatial distribution closely aligning with the pattern of population density distribution (Figure 6). The high-value regions were concentrated in the southern parts of the research region. Over time, the high-value regions for CS demand showed a trend towards centralization in urban centers and diffusion towards the edges, with some high-value areas gradually merging to form larger areas. Low-value regions were located in the northern parts of the research region; the population density in these areas is low and concentrated. Over the temporal dimension, the demand for CS demonstrated an overall upward trend. When viewed in terms of total demand, the CS demand increased by nearly 0.49 million tons over the past two decades, with an impressive growth rate of 333%.

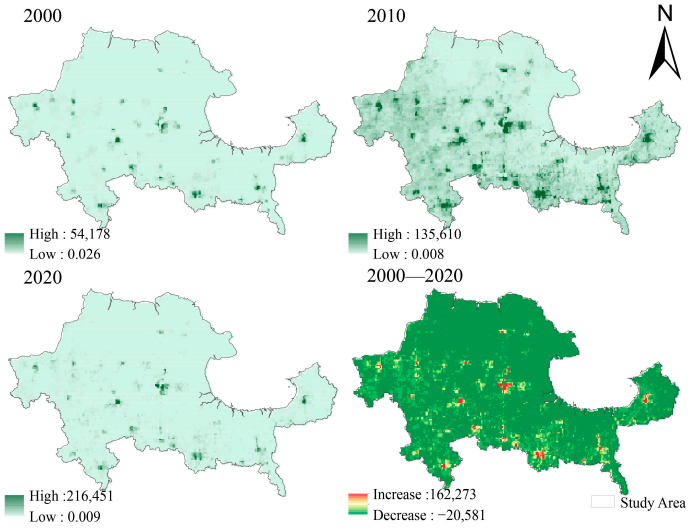


Figure 6. Spatial distribution of CS demand.

4.2. Supply–Demand Ratio of ES

The ES supply–demand ratio and the corresponding surplus-deficit relationship were calculated and illustrated in Figures 7 and 8. The average supply–demand ratios for habitat quality for the periods of 2000, 2010, and 2020 were −0.20, −0.29, and 0.01, respectively. The supply and demand for habitat quality have shown a slight improvement, with the supply–demand ratio index exhibiting a trend of initially decreasing and then increasing. Spatially, the regions with a deficit in habitat quality supply and demand were located in the southwestern part of the study area. The surplus regions were located in the northern and northeastern coastal parts of the research region.

The average supply–demand ratios for carbon sequestration services for the periods of 2000, 2010, and 2020 were 0.08, 0.02, and 0.005, respectively. Overall, the supply of carbon sequestration services has exceeded demand, with the supply and demand approaching equilibrium, but showing a general downward trend. Spatially, the regions with a deficit in carbon sequestration services were located in densely populated areas with intense human activity, such as urban construction land. The carbon sequestration surplus regions were predominantly found in areas of cropland, woodland, and grassland. These regions have relatively low human activity and high vegetation coverage. They were rich in above-ground organisms, below-ground soil, subsurface organisms, and dead organic matter. In the balance of supply and demand, these areas display a surplus, with supply exceeding demand, and were in a surplus state.

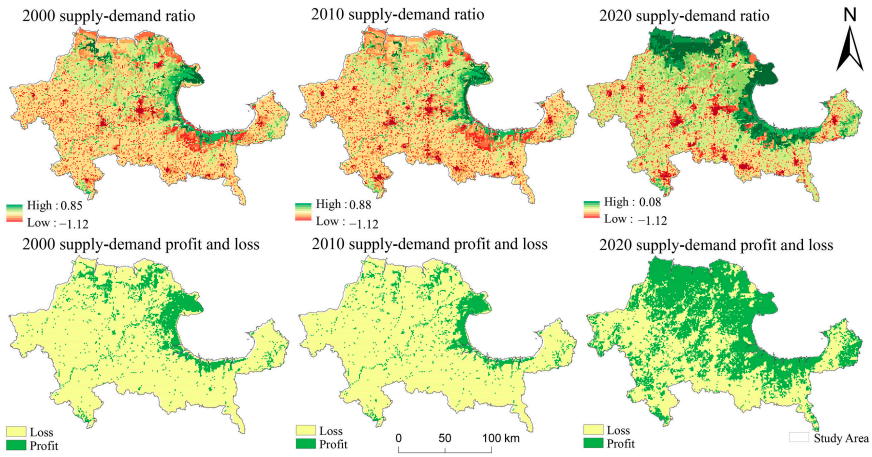


Figure 7. Supply–demand ratio and profit and loss of habitat quality service.

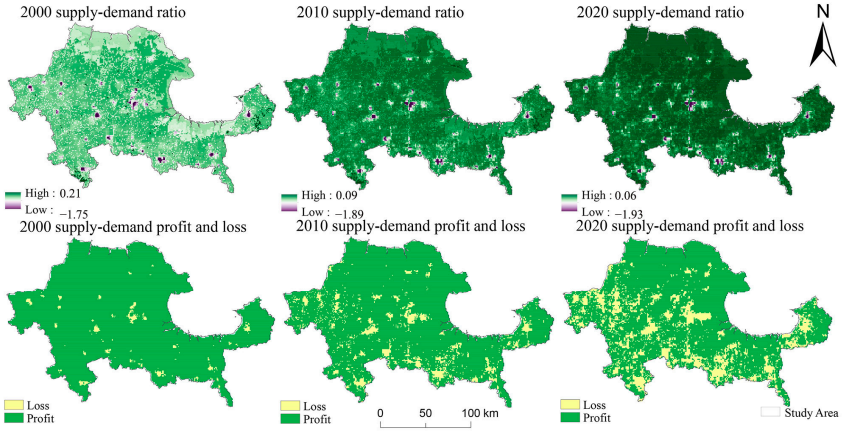


Figure 8. Supply–demand ratio and profit and loss of carbon sequestration service.

4.3. Analysis of Influencing Factors

The quantile regression results indicate that the factors affecting the supply–demand equilibrium at different quantiles exhibit variations (Table 2 and Figure 9). Within the low equilibrium range (quantiles ≤ 0.5), the proportions of woodland, grassland, water bodies, construction land, and unused land have a significant impact on the equilibrium. The proportions of construction land and unused land have a negative effect on the equilibrium, indicating that at low equilibrium levels, enhancing the protection and restoration of forest and grass ecosystems, as well as the continuous protection and restoration of wetlands, can contribute to promoting the balance between supply and demand in ecosystems. In the high equilibrium range (quantiles > 0.5), the negative impact of construction land proportion began to diminish. This could be attributed to the enhanced awareness of ecological protection among residents due to economic development and urbanization, accompanied by more comprehensive protection measures. Meanwhile, the negative impact of cropland proportion started to emerge, which may be attributed to the destruction of natural ecosystems and biodiversity caused by the expansion of cropland. Additionally, large areas of cropland can lead to soil erosion and degradation, affecting the health of the ecosystem and resulting in a diminishment in the supply capacity of HQ.

Table 2. Quantile estimation of the proportion of different types of land under the supply–demand equilibrium of habitat quality.

Explanatory Variable	OLS	Quantile				
		0.1	0.3	0.5	0.7	0.9
Proportion of cropland	−0.0104	0.0605	0.0207	−0.0282	−0.0503	−0.198 ***
	(0.0303)	(0.0603)	(0.0401)	(0.0363)	(0.0332)	(0.0428)
Proportion of woodland	0.438 ***	0.338 ***	0.421 ***	0.422 ***	0.431 ***	0.366 ***
	(0.0511)	(0.102)	(0.0676)	(0.0613)	(0.0561)	(0.0723)
Proportion of grassland	0.0371 ***	0.0520 ***	0.0476 ***	0.0358 ***	0.0310 ***	−0.00490
	(0.00894)	(0.0178)	(0.0118)	(0.0107)	(0.00981)	(0.0126)
Proportion of construction	−0.768 ***	−1.061 ***	−0.867 ***	−0.776 ***	−0.654 ***	−0.647 ***
	(0.0312)	(0.0621)	(0.0412)	(0.0374)	(0.0342)	(0.0441)
Proportion of unused land	−0.204 ***	−0.310 ***	−0.219 ***	−0.242 ***	−0.199 ***	−0.0102
	(0.0378)	(0.0754)	(0.0500)	(0.0453)	(0.0415)	(0.0535)
_cons	0.0229	−0.187 ***	−0.0574	0.0481	0.119 ***	0.334 ***
	(0.0378)	(0.0754)	(0.0500)	(0.0359)	(0.0329)	(0.0423)

Note: *** indicates a significance level of 1%, and the value in parentheses is the *t*-test result.

The OLS estimation results indicate that, except for construction land and unused land, all types of land use have a positive impact on the CS supply–demand equilibrium (Table 3 and Figure 10). Construction land has a significant negative impact on maintaining

the supply–demand balance, while grassland has a significant positive impact on the equilibrium of CS supply and demand. In the low equilibrium range (quantiles ≤ 0.5), the proportions of woodland, grassland, and water bodies play a crucial role in maintaining the balance, suggesting that at low equilibrium levels, efforts to enhance greening projects and protect wetlands can contribute to the balance between supply and demand for CS. In the high equilibrium range (quantiles > 0.5), the positive impact of water body proportion decreases, which may be attributed to the potential increase in dissolved organic carbon in water bodies due to the expansion of the water area. Additionally, the increase in the water body region could lead to an increase in biomass, such as algae and plankton, which upon death release significant amounts of carbon dioxide. This, in turn, could lead to a decrease in the supply capacity of CS and have a negative impact on ecosystem equilibrium.

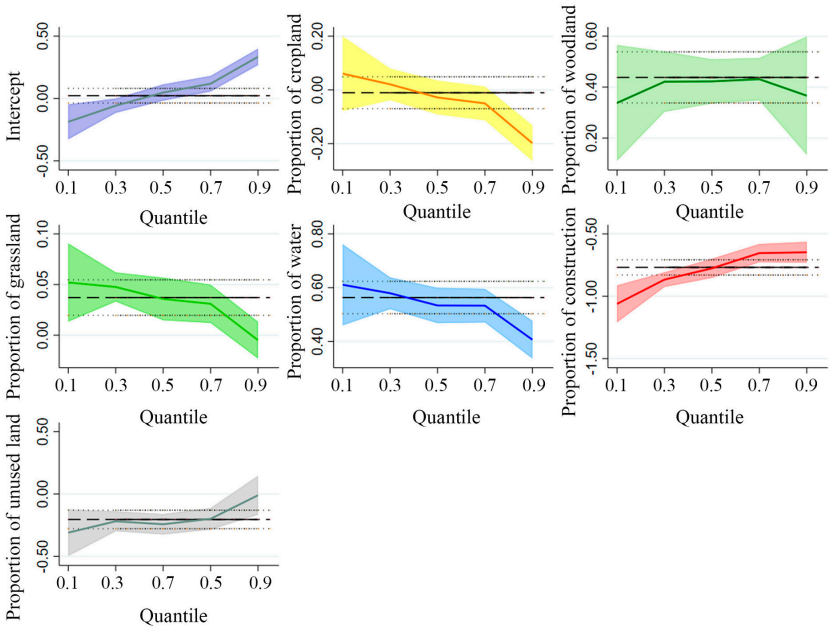


Figure 9. Parameter changes of various land use proportions under different quantiles in the quantile regression model (Habitat quality).

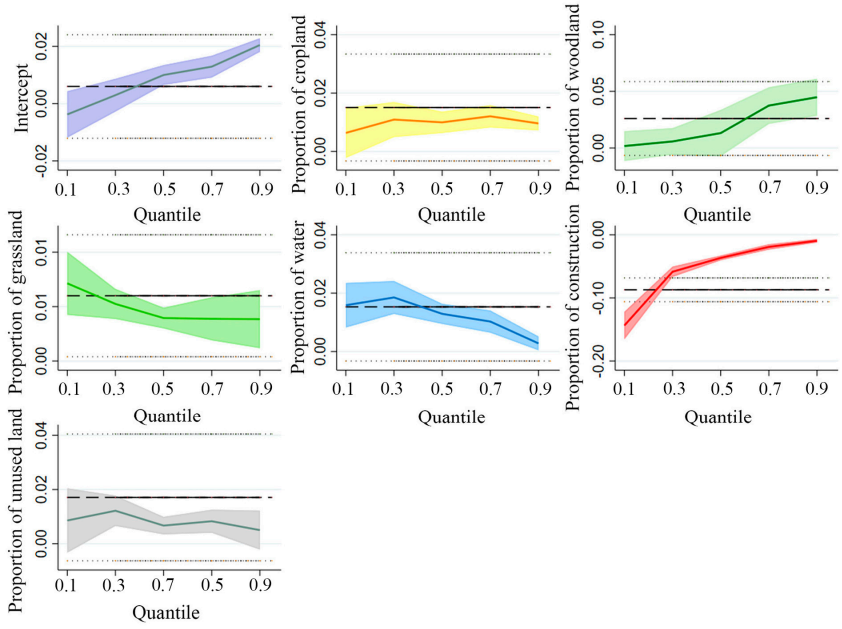


Figure 10. Parameter changes of various land use proportions under different quantiles in the quantile regression model (CS).

Table 3. Quantile estimation of the proportion of different types of land under the equilibrium level of supply and demand of carbon sequestration service.

Explanatory Variable	OLS	Quantile				
		0.1	0.3	0.5	0.7	0.9
Proportion of cropland	0.0151	0.00635	0.0109 **	0.0098 ***	0.0121 ***	0.00960 ***
	(0.00934)	(0.0156)	(0.00461)	(0.00314)	(0.00256)	(0.00166)
Proportion of woodland	0.0260	0.00172	0.00579	0.0131 **	0.0374 ***	0.0448 ***
	(0.0166)	(0.0278)	(0.00823)	(0.00561)	(0.00456)	(0.00296)
Proportion of grassland	0.00599 ***	0.00714	0.00525 ***	0.00395 ***	0.00388 ***	0.00385 ***
	(0.00286)	(0.00478)	(0.00141)	(0.000963)	(0.000783)	(0.000509)
Proportion of construction	−0.0872 ***	−0.144 ***	−0.0585 ***	−0.0366 ***	−0.0192 ***	−0.00947 ***
	(0.00963)	(0.0161)	(0.00476)	(0.00324)	(0.00263)	(0.0171)
Proportion of unused land	0.0171	0.00857	0.0122 **	0.00669 *	0.00830 **	0.00502 **
	(0.0199)	(0.0199)	(0.00590)	(0.00402)	(0.00327)	(0.00212)
_cons	0.00600	−0.00377	0.00296	0.0100 ***	0.0129 ***	0.0205 ***
	(0.00922)	(0.0154)	(0.00456)	(0.00311)	(0.00252)	(0.001643)

Note: *, **, *** indicate 10%, 5%, and 1% significance levels, respectively, with *t*-test results in parentheses.

4.4. Hot Spot Analysis

The spatial distribution of hot spots for the HQ and CS supply–demand ratio in 2020 is depicted in Figures 11 and 12. The cold spots of HQ were distributed in the Bincheng District, Qingyun County, Xinyang County, and Zouping County. The hot spots, on the other hand, were concentrated in the northern and northeastern coastal towns of the research region, connecting to contiguous areas, roughly forming a spatial distribution pattern of "hot" in the north and "cold" in the south. The cold spots of the CS supply–demand ratio were distributed in the Bincheng District (Figure 12); the hot spots were mainly concentrated in Wudi County, Zhanhua County, and Hekou County, roughly forming a spatial distribution pattern of "hot" in the north and "cold" in the center.

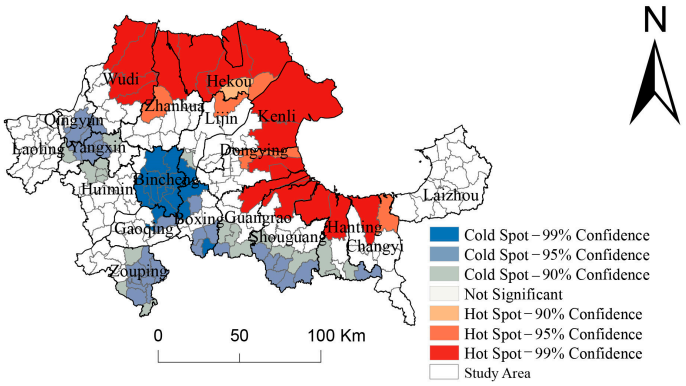


Figure 11. Spatial distribution of hot and cold spots for habitat quality service.

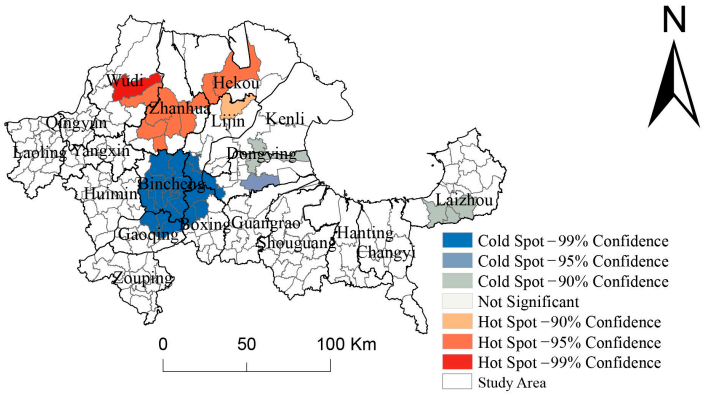


Figure 12. Spatial distribution of hot and cold spots for carbon sequestration service.

4.5. Simulation of ES Flow

4.5.1. HQ Flow

(1) Supply and demand area identification

The connectivity paths between the supply and demand regions for habitat quality services in 2020 are illustrated in Figure 13, revealing the presence of one supply region and four demand regions. The supply region, located in the northeastern part of the study area (northeast supply region, 9040.88 km^2), was formed by multiple coastal towns in the cities of Binzhou, Dongying, and Weifang, connecting to form a contiguous area. The demand region can be divided into four sections: the northwestern demand region, the central demand region, the southern demand region, and the southeastern demand region. The area of the western demand region is 631.07 km^2, the central demand region is 1489.13 km^2, the southern demand region is 320.80 km^2, and the southeastern demand region is 523.89 km^2.

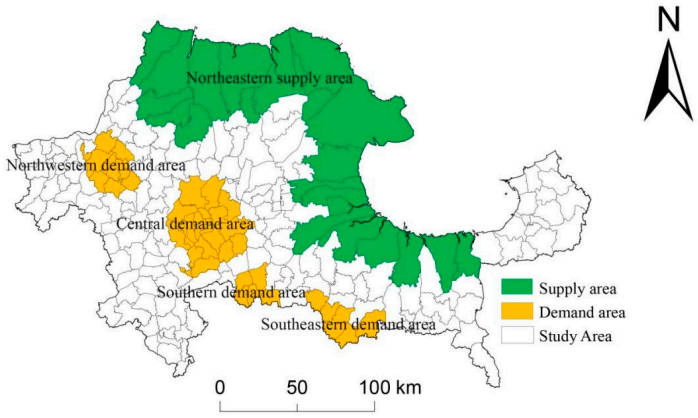


Figure 13. Spatial distribution of HQ supply and demand regions.

(2) Ecological resistance surface construction

The MCR analysis found that woodland and grassland areas had lower resistance values, while areas of construction and unused land had higher resistance values (Figure 14). The basic resistance surface was set according to elevation and slope, with higher values corresponding to higher elevations and steeper slopes. Additionally, the basic resistance surface was calculated based on the NDVI, with the northeastern coastal region having low vegetation coverage, an abundance of construction and unused land, and high human activity interference, resulting in higher resistance values. In contrast, the southwestern region has a more extensive distribution of cropland, higher vegetation coverage, and thus lower resistance values. The resistance surface was also established based on the distance from rivers, with lower resistance values in proximity to water bodies. Furthermore, the resistance surface was computed and identified based on the distance from roads, where areas with frequent human activity have higher resistance values.

The comprehensive resistance surface was derived through the application of weighted operations to each resistance factor (Figure 15). Across the region, the predominant resistance levels were low to moderate, with the lowest resistance values predominantly found in areas of woodland, grassland, cropland, and in the vicinity of the river system. These areas were characterized by minimal human interference, fostering an environment conducive to ecological integrity. In contrast, the highest resistance values were predominantly associated with construction land and road networks, where human activity is intense and vegetation cover is notably sparse.

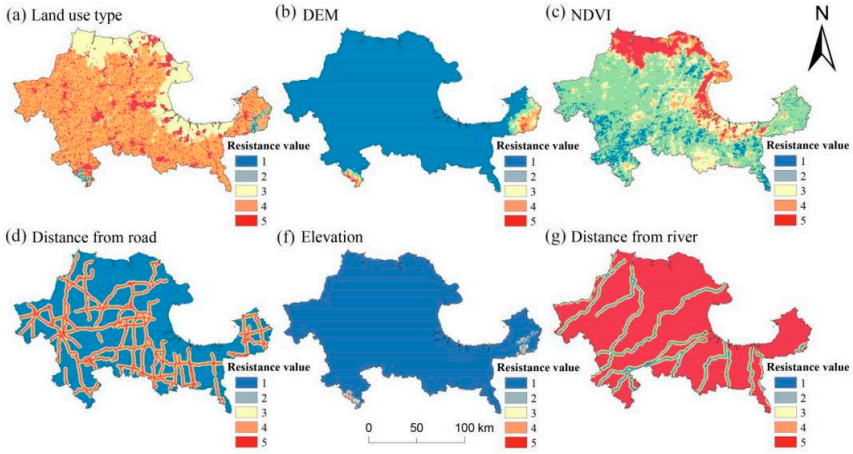


Figure 14. Classification of ecological resistance factors.

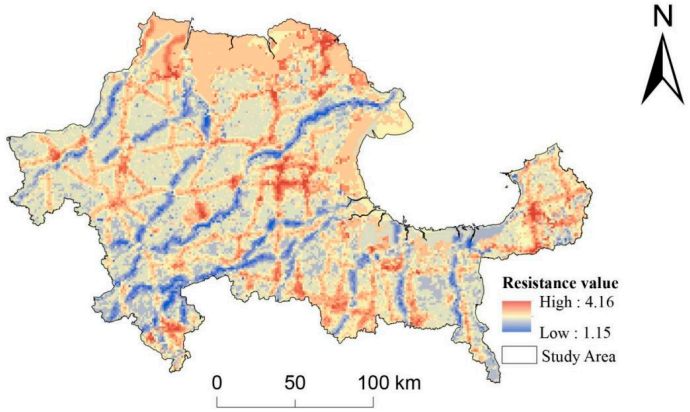


Figure 15. Spatial distribution of resistance surface.

(3) Supply and demand area connection path extraction

The demand areas for HQ were located in the southern part of the study area, while the research regions were situated in the northeastern coastal region. The flow paths of HQ connect these main demand and supply regions. Based on the location relationships between the supply and demand regions and the comprehensive resistance surface, the connection paths between the supply and demand regions were constructed using linkage mapper software (Plugin for ArcGIS 10.8), as shown in Figure 16. It can be found that the flow paths of HQ were distributed in the central part of the study area in 2020, with the supply and demand regions connected by cropland, water bodies, and grasslands (Table 4). A total of 25 ecological corridors were identified, with a total length of 617.28 km and an average length of 24.69 km. The longest corridor was 45.38 km, and the shortest was 15.14 km, all of which significantly contributed to the ecological connectivity of the research region.

Table 4. Distribution of ES flow corridors for habitat quality.

	Northwestern Demand Area	Central Demand Area	Southern Demand Area	Southeastern Demand Area
Number of corridors	6	9	2	8
Average length/km	21.60	28.25	20.19	24.13
Total length/km	129.58	254.27	40.38	193.05

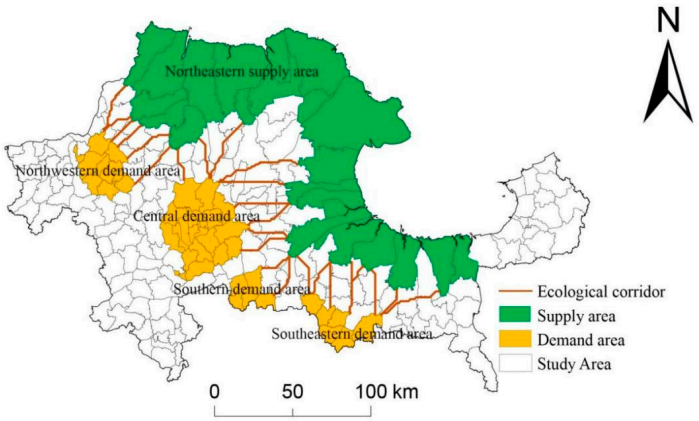


Figure 16. Spatial distribution of ecological corridors.

(4) Ecological pinch point

Ecological pinch points exhibited high current density values and low ecological resistance, serving as the core areas connecting supply and demand regions. They must be actively improved and protected to ensure their stable functionality in maintaining the connectivity of corridors. In 2020, the habitat quality service flow pattern featured 30 corridor pinch points. These ecological pinch points were evenly distributed along the connecting corridors between the supply and demand regions, with the areas being dominated by cropland and water bodies. It is necessary to enhance their protection to provide a safeguard for the ecological flow within the corridors (Figure 17).

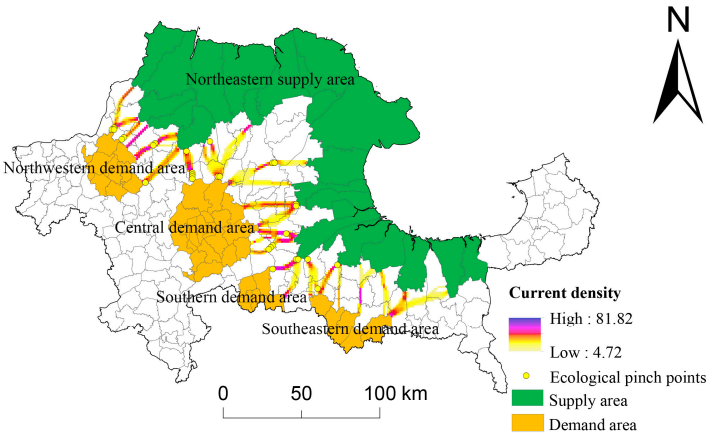


Figure 17. Spatial distribution of current density of ecological corridor and pinch points.

(5) Ecological barrier point

Utilizing search radii of 1000 m, 2000 m, 3000 m, 4000 m, and 5000 m, the percentage improvement in scores within the entire mobile search window was divided into five intervals using the natural breakpoint method, with the highest interval designated as an obstacle point. A comparison of the obstacle point identification results under different search radii revealed that the recognition results at a radius of 2000 m were essentially consistent with those at radii of 3000 m, 4000 m, and 5000 m. Consequently, a detection radius of 2000 m was chosen to identify ecological obstacle areas. In the year 2020, the study area was found to harbor a total of 98 obstacle points, as illustrated in Figure 18. These points were largely situated between the central and southeastern demand zones and the northeastern supply region. They were especially concentrated in specific areas, with land predominantly used for construction and agricultural purposes. The emergence of these ecological obstacle points stemmed from human interference, rendering them vulnerable nodes within the ecological network. To enhance corridor connectivity and facilitate a more

cohesive flow between ecological supply and demand zones, it is crucial to focus on the restoration and rehabilitation of these fragile areas.

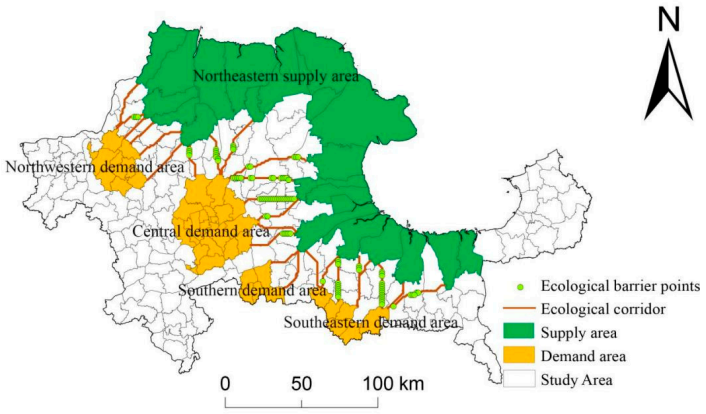


Figure 18. Spatial distribution of ecological barriers.

(6) Habitat quality service flow patterns

To analyze the spatial flow of supply and demand of habitat quality services in the research region, based on the supply and demand zones of habitat quality services and integrated resistance surfaces, circuit corridors were used to connect the major supply zones with the main demand zones and important ecological nodes of the habitat quality service flow were extracted, and in this way, the pattern of the flow of habitat quality services was constructed and derived with the demand zones and supply zones as the ecological barriers (Figure 19). A total of 25 ecological corridors, 30 ecological pinch points, and 98 ecological barrier points were identified in this study.

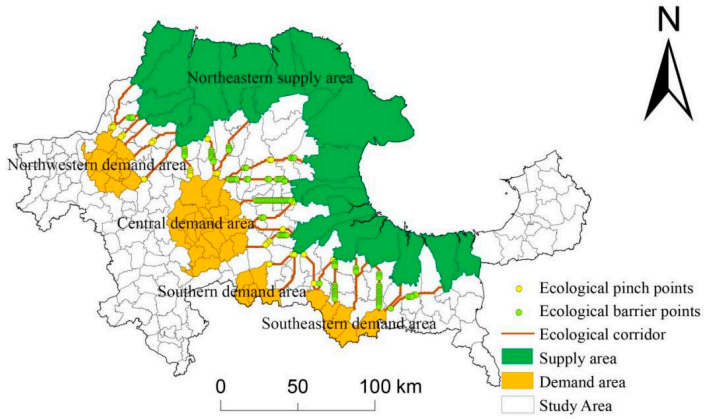


Figure 19. Habitat quality service flow.

In the habitat quality service flow pattern of 2020, ecological pinch points were predominantly distributed in Xuyuanzi Town in Qingyun County, Huangsheng Town in Zhanhua County, Huaguan Town in Guangrao County, and Yanwo Town in Lijin County. As depicted in the remote sensing image in Figure 20, letters A, B, C, and D represent the distribution of ecological pinch points in Huangsheng Town, Xuyuanzi Town, Yanwo Town, and Huaguan Town, respectively. Ecological pinch points were often found in suburban or rural areas, distributed in cropland and near water bodies. Therefore, it is advisable to increase the green area along riverbanks and to conduct ecological transformation of cropland, plant artificial forest, and construct biological corridors to enhance ecological connectivity.

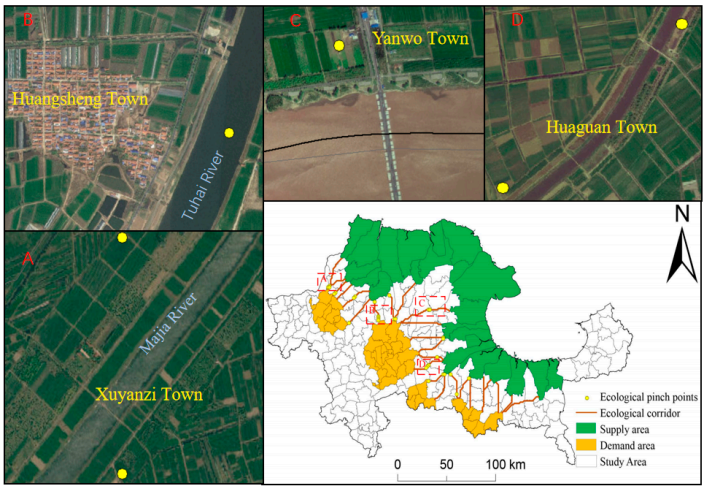


Figure 20. Local detail map of ecological pinch points. (**A**) The ecological pinch points in the Xuyanzi Town (**B**) The ecological pinch points in the Huangsheng Town (**C**) The ecological pinch points in the Yanwo Town (**D**) The ecological pinch points in the Huaguan Town.

As illustrated by the habitat quality service flow pattern in 2020 (Figure 19), ecological barriers were distributed in Fuguo Sub-district and Botou Sub-district in Zhanhua County, Haojia Town, Xindian Sub-district, and Huanghe Road Sub-district in Dongying District, Tianliu Sub-district, Gucheng Sub-district, Houzhen, and Luocheng Sub-district in Shouguang City. As shown in the remote sensing image in Figure 21, letters A, B, C, and D depict the distribution of ecological barriers in Fugu Sub-district, Huanghe Road Sub-district, Tianliu Sub-district, Gucheng Sub-district, and Houzhen, respectively. From the current status of barriers, it is observed that barriers were located in the central areas of major urban centers, with land use classified as construction land. This represents a conflict between urban development and ecological protection. Therefore, during the process of urban construction, it is essential to promote the timely construction of green belts to enhance urban greening levels and transform high-resistance ecological barriers into low-resistance ecological pinch points.

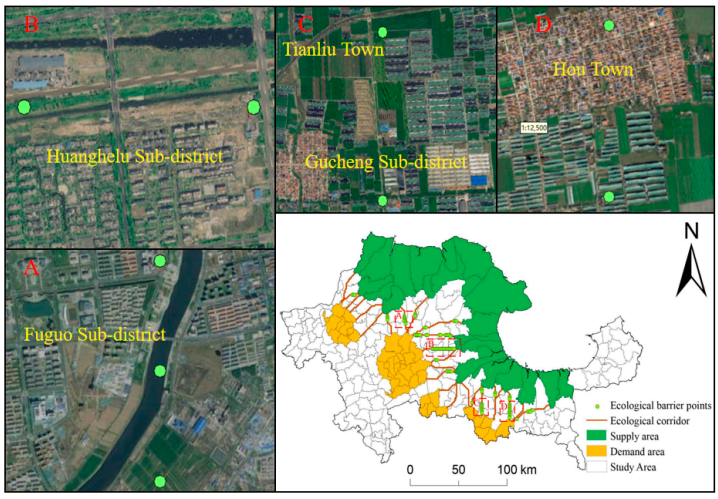


Figure 21. Local detail map of ecological barriers. (**A**) The ecological barriers in the Fuguo Sub–district (**B**) The ecological barriers in the Huanghelu Sub–district (**C**) The ecological barriers in the Tianliu Town and Gucheng Sub–district (**D**) The ecological barriers in the Hou Town.

4.5.2. CS Flow

(1) Supply and demand area identification

The hot spot analysis on the supply–demand ratio of CS was utilized to identify the demand and supply regions. These regions were then connected along the prevailing wind direction, and the intensity of the CS flow was quantitatively analyzed using the breakpoint model and the field strength model. This analysis determined the direction and magnitude of the carbon sequestration service flow between the supply and demand regions. As depicted in Figure 22, the supply and demand regions for CS in 2020 were located. The study area comprised one supply region and one demand region. The supply region was situated in the northern part of the research region and was composed of multiple towns in Wudi County, Zhanhua County, and Hekou District. The demand region was located in the central part of the research region and was made up of multiple towns in Bincheng District, Lijin County, Dongying District, Boxing County, and Gaoqing County, with most of the area being within Bincheng District. The area of the demand region was 1745.32 km^2, and the area of the supply region was 1777.62 km^2.

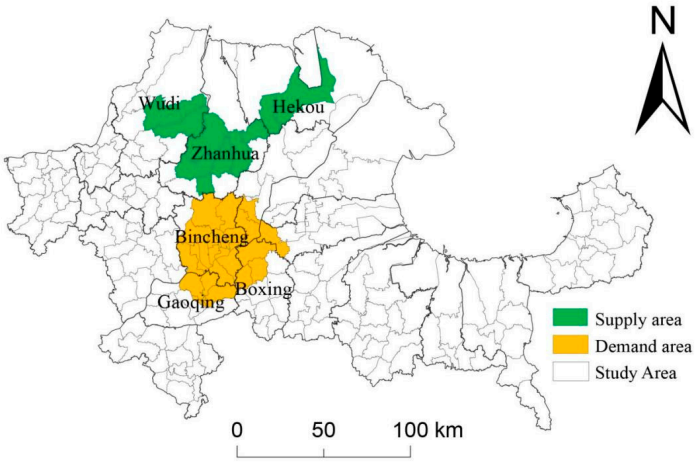


Figure 22. Spatial distribution of supply and demand areas for carbon sequestration service.

(2) Pattern of CS flow

The flow of CS was formed by connecting the supply and demand areas of CS with the annual highest frequency wind direction as a path. Using the inverse distance weight interpolation algorithm, the interpolation analysis results of wind direction data were obtained. In 2020, the distribution of carbon sequestration service, as depicted in Figure 23, revealed that the demand areas were found in Bincheng District, Boxing County, and Gaoqing County. The total carbon storage stood at 5.457 million tons, whereas the total carbon emissions amounted to 5.989 million tons, resulting in a supply–demand deficit of 532,800 tons. The supply areas were situated in Wudi County, Zhanhua County, and Hekou District, with a total carbon storage of 5.624 million tons and a total carbon emission of 2.252 million tons, leading to a supply–demand surplus of 3.372 million tons. The excess carbon emissions from the demand areas were transported towards the north to the supply areas for carbon sequestration, following the direction of the southwest wind.

(3) Radius and scope of CS circulation

The ES flow radius of each supply zone was calculated based on the fracture point formula, and the flow range from each supply zone to each demand zone was obtained using the buffering tool. As shown in Table 5, the radius of carbon sequestration service flow in each supply zone in 2020 was between 6.52 and 89.97 km, among which the maximum flow radius of the supply area was between 33.45 and 89.97 km, and the farthest area that could be reached by the carbon sequestration service flow was located in Qintian Sub-district and Xiaoying Sub-district in Bincheng District, while the minimum flow radius

of the supply area was between 6.52 and 39.01 km, and the nearest area of the carbon sequestration service flow was located in Qintian Sub-district and Xiaoying Sub-district in Bincheng District. The closest area of the supply zone was located in the periphery of each supply zone. Due to the difference in the level of ESs between the supply area and the demand area and the distance between the two areas, the supply area could not satisfy the carbon sequestration demand of all the demand areas.

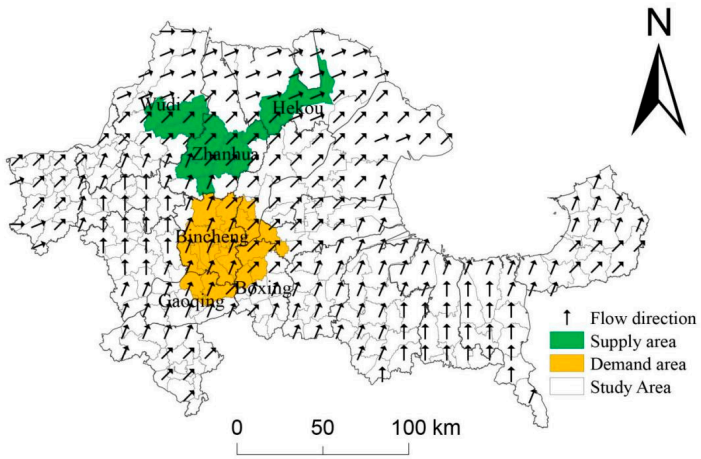


Figure 23. Carbon sequestration service flow in the study area.

Table 5. ES circulation radius.

Supply Area	Maximum Flow Radius (km)	Maximum Radius of Reachable Area	Minimum Flow Radius (km)	Minimum Radius Reachable Area
Yihe Town, Hekou County	73.80	Qingtian Sub-district, Bincheng County	24.10	Fuyuan Sub-district, Zhanhua County
Liubao Town, Wudi County	69.10	Shizhong Sub-district, Bincheng County	31.31	Fuguo Sub-district, Zhanhua County
Huangsheng Town, Zhanhua County	3345	Longju Town, Dongying County	6.52	Binbei Sub-district, Bincheng District
Xi Xiaowang Town, Wudi County	61.09	Xiaoying Sub-district, Bincheng County	24.96	Huangsheng Town, Zhanhua County
Xiahe Town, Zhanhua County	63.61	Qingtian Sub-district, Bincheng County	17.64	Hekou Sub-district, Hekou County
Xiwa Town, Zhanhua County	41.56	Qiaozhuang Town, Boxing County	10.67	Fengjia Town, Zhanhua County
Fengjia Town, Zhanhua County	55.08	Xiaoying Sub-district, Bincheng County	20.47	Xihe Township, Zhanhua County
Fuyuan Sub-district, Zhanhua County	51.47	Pangjia Town, Boxing County	11.76	Fengjia Town, Zhanhua County
Hekou Sub-district, Hekou County	89.97	Lizhe Sub-district, Bincheng County	39.01	Fuyuan Sub-district, Zhanhua County

(4) Intensity of CS flow

The intensity of CS flow was calculated based on the field strength formula and the radiation area of the supply area to the demand area. As shown in Figure 24, the main supply area of ES flow was located in Fengjia Town of Zhanhua County, Hekou Sub-district of Hekou District, and Xixiaowang Town of Wudi County, while the main demand area was located in Binbei Sub-district of Bincheng County, Qinhuangtai Town, and Yangliuxue Town. The northern supply area can receive the demand for carbon sequestration from 20 townships with a total flow of 369,500 t. The demand for carbon sequestration services in Changjia Town, Tangfang Town, and Luhu Sub-district in Gaocheng County cannot be met.

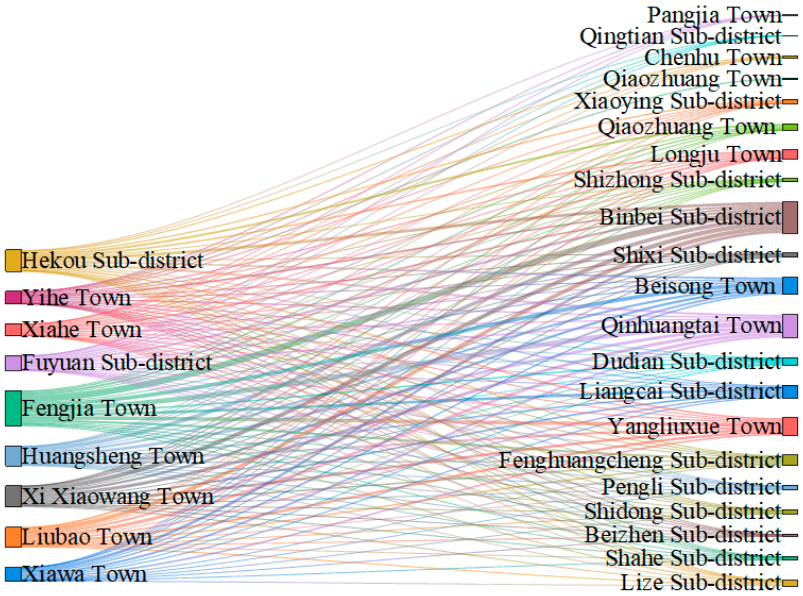


Figure 24. CS flow between the CS supply area (left axis) and the CS demand area (right axis).

5. Discussion

5.1. Selection of ESs

In pursuit of greater economic benefits, the study area has resorted to extensive use of fossil fuels for energy production and transportation, leading to a rise in atmospheric carbon dioxide concentrations and exacerbating the greenhouse effect. This is further compounded by the acceleration of urbanization. The extensive conversion of woodland for agriculture and urban development has also severely disrupted regional biodiversity. The CS and HQ effectively reflect the high-intensity human activities' demands on ecosystems. Consequently, this study, aiming for the synergistic development of the ecological environment and economy, has chosen carbon sequestration and habitat quality as the ESs to model and study. Moreover, while ESs were diverse, certain indirect services, such as those provided by insects, birds, and butterflies during pollen dispersal, were challenging to simulate and quantify. Therefore, this paper has selected habitat quality and carbon sequestration services, which were more typical and easier to quantify. Although this study focused on these two classic ESs, other service flows can be similarly categorized and extended within the suggested framework. For instance, crop production services can be transported through road networks, water production services can be conveyed through river networks and soil conservation can be transmitted through vegetation and river systems [41].

5.2. Supply and Demand Patterns

Previous studies indicated that the provision and utilization of habitat quality services and carbon sequestration services exhibited distinct patterns within the study area [24,42]. Specifically, areas experiencing a shortfall in both carbon sequestration and habitat quality services were predominantly found in the southwestern region, where the land use was predominantly characterized by construction and agricultural activities. In contrast, regions surplus in habitat quality services were situated in the coastal towns of the northern and northeastern parts of the research region. Additionally, areas with an excess of carbon sequestration services were mainly associated with land cover types such as croplands, woodlands, and grasslands.

To gain a more comprehensive understanding of the supply and demand of ESs in the study area, this study normalized and spatially overlaid the supply–demand ratios of CS and HQ. This approach facilitated the construction of the comprehensive ES supply–demand pattern for the research region, which was further refined through cold and hot

spot analysis to establish the distribution pattern of the comprehensive ES cold and hot spots. The supply–demand ratios of the comprehensive ESs for the years 2000, 2010, and 2020 were depicted in Figure 25. The low-value regions of the comprehensive ES supply–demand ratio were concentrated in the southern urban built-up areas of the study area (Shengcheng Sub-district in Shouguang City, Gaoxin Sub-district in Zouping County, Xindian Sub-district in Dongying District, Shizhong Sub-district in Bincheng, and Xincheng Sub-district in Yangxin County). Conversely, the high-value regions were distributed in the northern and northeastern coastal towns of the study area (Wudi County, Zhanhua County, Hekou District, Kenli County, and Dongying District), forming a spatial distribution pattern of "hot" in the north and "cold" in the south.

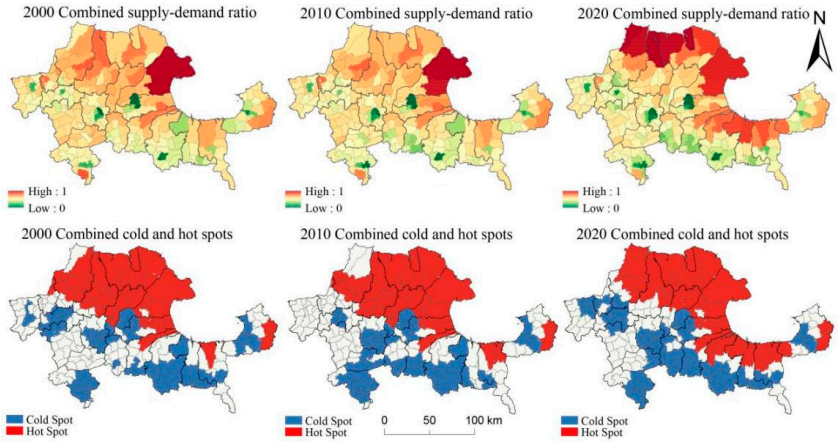


Figure 25. Supply and demand patterns of integrated ESs within the research locale.

An examination of the cold and hot spot distribution patterns revealed that over the past two decades, the hot spots in the supply–demand ratio of ESs have initially decreased and then increased, with the overall change being relatively insignificant. The comprehensive hot spots were predominantly located in the estuarine area, Kenli County, Wudi County, Lijin County, and Zhanhua County. By 2020, the hot spot areas in these counties accounted for 99.12%, 82.68%, 70.49%, 69.20%, and 64.09% of their respective county areas, respectively. In contrast, the cold spots in the comprehensive supply–demand ratio of ESs across the three periods have generally increased. The comprehensive cold spots were situated in Boxing County, Zouping County, Bincheng District, and Yangxin County. By 2020, the cold spot areas in these counties accounted for 80.95%, 62.87%, 61.14%, and 60.70% of their respective county areas, respectively.

5.3. Exploring Land Use-Ecosystem Service Balance

Based on previous research, we have come to understand that the structure of land use plays a critical role in the equilibrium of supply and demand for ES. In states of low equilibrium for habitat quality services, the expansion of forested, grassland, and wetland areas has significantly enhanced ecosystem health. However, as urbanization intensifies, the continuous expansion of construction land has hurt this balance. For instance, the research by Shaikh and others confirmed that urbanization has altered forest cover, disrupted biodiversity, and negatively affected ecosystem services [43]. When the supply and demand for ES attain a superior state of balance, the adverse effects of excessive expansion of cultivated land become particularly pronounced. For example, studies by Wang et al. have shown that the conversion of wetlands to cropland dramatically changes the structure and function of ecosystems, leading to a substantial decrease in the supply of ES and causing significant harm to human well-being [44].

At low equilibrium levels of carbon sequestration services, the synergistic effects of forests, grasslands, and water bodies are essential in preserving the equilibrium of carbon sink systems. As revealed by the research of Wang et al., fully leveraging the

carbon sequestration capabilities of forests, grasslands, and soils can significantly enhance a region's capacity to act as a carbon sink, thereby maintaining the balance of the carbon cycle within ecosystems [45]. However, when the supply and demand for CS reach a high level of equilibrium, the positive impact of water bodies on the balance diminishes. Therefore, strategic land management planning and environmental preservation strategies are crucial for maintaining the equilibrium of ES.

5.4. Policy Implications

Upon conducting a thorough investigation and analysis of the CS flow, this study reveals that while the current supply areas can partially fulfill the carbon sequestration needs of certain regions, the constraints imposed by geographical location and supply capabilities have precluded the possibility of universal coverage across all demand areas. The imbalance between supply and demand for carbon sequestration services is especially acute in densely populated, highly industrialized regions devoid of extensive ecological resources, such as Bincheng County, Gaocheng County, and Boxing County. Drawing on the analysis of how land-use patterns affect the availability and demand for CS, we acknowledge the critical importance of safeguarding and increasing the expanse of green vegetation, including forests and grasslands, as a pivotal strategy to bolster the carbon sink capability.

Concurrently, the stringent regulation of construction land expansion and the prudent management of water resources are indispensable for preserving and amplifying the effectiveness of regional carbon sequestration efforts. Consequently, we propose the designation of Bincheng, Gaocheng, and Boxing counties as focal zones for the augmentation of carbon sinks. These areas should prioritize land-conservation strategies, advance urban greening initiatives, and refine spatial planning to elevate land-use efficiency and intensify the carbon sequestration capacity of their urban environments. Furthermore, there is an imperative to champion the development of an ecological compensation framework to provide a robust financial underpinning for the execution of carbon sink initiatives. Additionally, it is essential to reinforce interregional partnerships and foster enduring collaborative ties with supplying regions to secure a consistent flow of carbon credits. Moreover, taking a proactive approach to facilitating the exchange of insights and disseminating best practices across regions is vital to fostering collective advancement.

The national plan for environmental conservation and high-quality development of the Yellow River Delta clearly advocates a modern path of ecological priority and green development. Safeguarding the ecological security of the estuarine delta and enhancing the functionality of ESs were of the utmost priority. The supply areas for habitat quality were situated in the coastal regions of the northern and northeastern parts of the study area, where reserves rich in unique ecological resources such as the confluence of rivers and the sea, ecological wetlands, rare and endangered bird species, and coastal tidal flat landscapes. These areas possess well-developed ecological functions and a pronounced ecological barrier role. By simulating the dynamics of habitat quality service flows, this investigation pinpointed a network of 25 essential ecological corridors, 30 pivotal ecological pinch points, and 98 ecological barrier points within the research zone. These ecological corridors serve as vital conduits for species migration, facilitating the seamless transfer of habitat-quality services throughout the ecosystem. Ecological pinch points are predominantly situated at the urban-rural fringe or within rural landscapes, flanking agricultural fields and water bodies. They act as critical connectors, facilitating the uninterrupted flow of habitat quality services. Conversely, ecological barrier points are found within the dense fabric of urbanized regions, underscoring the substantial barrier that urbanization poses to the seamless movement and connectivity of ecological processes. Drawing insight from the driving forces behind habitat quality service flows, we are deeply conscious of the imperative to protect and rehabilitate forest, grassland, and wetland ecosystems. Furthermore, we are on high alert to the potential harmful effects that unchecked agricultural expansion may have on the health of ecosystems and the diversity of species. To address these concerns,

we propose the following recommendations: reinforce the protection and restoration of ecological pinch points in suburban and rural areas and rigorously curtail the unregulated expansion of construction and unused land; enhance the service functions of ecosystems through measures such as afforestation, grassland rehabilitation, and wetland conservation; elevate the standards of arable land management and protection by implementing policies aimed at preventing the indiscriminate expansion of farmland and mitigating damage to natural ecosystems; and utilize remote sensing technology and big data analytics to conduct regular monitoring and evaluation of the effects of land use transformations on the movement of ES.

5.5. Limitations

This research offers fresh insights into the correlation between ecological security and national territorial planning. The disparity in the distribution of ES supply and demand leads to the movement of services from regions of abundance to those experiencing scarcity, prompting an investigation into the dynamics of ES flows. [46]. However, this study has limitations. This study employed two types of ESs for analysis and investigation. Future studies can comprehensively consider the supply, flow, flow direction, flow rate, dissipation, and consumption changes, as well as the direction of different types of ESs and the scope of supply, etc., analyze the impacts of ESs on the regions involved in the process of ES transfer, reveal the loss and decay law of ESs in the process of ES transfer, and achieve the exploration of the spatial transfer law of ESs across the scales, regions, and borders [47]. Given the challenge of directly obtaining detailed carbon emission data for each county within the study area, this study adopted an alternative estimation approach. It relies on the comprehensive carbon emission data of Shandong Province to extrapolate the carbon emissions for the research area. Considering the similarities in economic activities and industrial structures within Shandong Province, and particularly since the study area is a pivotal economic sector, its industrial structure and energy consumption patterns were highly correlated with the overall provincial trends. In contrast to the carbon emission data for individual counties, which is difficult to collect directly, the aggregate carbon emission data for Shandong Province is currently not only more accessible but also typically more comprehensive and systematic. Further study will explore the accessibility of direct accounting methods to ensure the higher accuracy of carbon emission. In this study, we employed the least resistance accumulation model and the Breakpoint model to simulate the flow processes of HQ and CS, respectively. However, it is important to note that many of these models are based on simplifying assumptions, such as assuming uniform diffusion of carbon sequestration services from the source. This assumption may overlook the complexity and non-uniformity present in actual ecological processes. Additionally, these models only provide a static simulation of service flow at a single moment, while ecosystem services are constantly evolving over time. The temporal dynamics of this process may not be adequately captured by the model's time-dimensional dynamics. Furthermore, land utilization patterns have a significant impact on the flow of CS and HQ. Moreover, the resolution of land use data plays a crucial role in determining potential biases in study outcomes. Therefore, future research should utilize data with improved resolution to conduct detailed observations of ecosystem service flows over multiple years. This approach will enable more accurate monitoring of changes in ecosystem services at finer levels.

6. Conclusions

This study integrated multi-modeling methods and socio-economic data to quantify habitat quality and carbon sequestration service supply and demand in an ecological economic zone from 2000 to 2020. The ES supply–demand ratio (ESDR) model, quantile regression, and hot and cold spot analyses were used to map service imbalances at the township level and assess land use patterns' effects. The supply and demand zones were

found and mapped, with circuit corridors and wind directions as key pathways, defining flow dynamics and ecological nodes. The key findings include the following:

(1) The supply of the ESs generally increased, with a significant rise in demand for carbon sequestration services and a downward momentum in habitat quality service demand.

(2) Spatial mismatches were found between the supply and demand of ESs. Low-value service areas were found in thickly settled cityscapes in the southwestern portion of the research zone, high habitat quality service value areas were located in the coastal regions, and high carbon sequestration service values were in croplands, forests, and grasslands.

(3) The land use structure has a complex impact on the balance of supply and demand for ES. When the balance of ES supply and demand is low, forests, grasslands, and wetlands play a positive role in maintaining ecosystem health and carbon sequestration equilibrium. Conversely, in the high balance range, the expansion of farmland exerts a significant negative impact on ES, while simultaneously, the positive effects of water bodies on ES diminish.

(4) Habitat quality and carbon sequestration services show different hot and cold spot distribution patterns. Habitat quality cold spots were mainly in the south, with hot spots in the north and northeast, forming a 'hot north, cold south' pattern. For carbon sequestration, a 'hot north, cold center' pattern was created.

(5) Habitat quality service has eased the supply–demand gap, identifying 25 corridors, 30 pinch points, and 98 barriers. Carbon sequestration partially balanced the deficit, with a 532,800-ton shortfall in the main demand area and a 3,372,100-ton surplus in the supply zone. Northern supply met 20 demand areas, but Changjia, Tangfang, and Luhu in Gaoqing had unmet needs, showing a 369,500-ton surplus in supply and a 532,800-ton deficit in demand.

The policy implications of this study were to strengthen the supply of carbon sequestration services, promote carbon neutrality, protect habitat quality, and optimize the flow of services. The results of this research offer theoretical direction and practical reference for the optimization of ESs in the efficient ecological economic zone of the Yellow River Delta and beyond, enhance the foundation for decision-making in regional environmental conservation and sustainable progress., and contribute a new perspective and approach to examining of ES flow.

Author Contributions: Conceptualization, W.Q. and X.Y.; Methodology, W.L.; Software, Q.S.; Validation, Q.S.; Formal analysis, Q.S.; Investigation, X.M.; Data curation, X.M.; Writing—original draft, W.L. and X.Y.; Writing—review & editing, X.Y.; Funding acquisition, X.Y. All authors have read and agreed to the published version of the manuscript.

Funding: This study was supported by the construction of spatial optimization model for territory (140-381181), the evaluation and optimization of collective profit-making construction land (010-381180), and the National Key Research and Development Program of China (2022YFC3204404). The supporters have no role in the study design, data collection, decision to publish, or preparation of the article.

Data Availability Statement: The data used in this study are available from the corresponding author upon reasonable request.

Acknowledgments: The authors would like to thank the anonymous reviews for their constructive suggestions and comments.

Conflicts of Interest: The authors declare no conflicts of interest.

Abbreviations

Ecosystem Service (ES); Habitat quality service (HQ); Carbon sequestration service (CS).

References

1. Feurer, M.; Rueff, H.; Celio, E.; Heinimann, A.; Blaser, J.; Htun, A.M.; Zaehringer, J.G. Regional scale mapping of ecosystem services supply, demand, flow and mismatches in Southern Myanmar. *Ecosyst. Serv.* **2021**, *52*, 101363. [CrossRef]
2. Zhai, T.; Wang, J.; Jin, Z.; Qi, Y.; Fang, Y.; Liu, J. Did improvements of ecosystem services supply-demand imbalance change environmental spatial injustices? *Ecol. Indic.* **2020**, *111*, 106068. [CrossRef]
3. Meng, Q.; Zhang, L.; Wei, H.; Cai, E.; Xue, D.; Liu, M. Linking Ecosystem Service Supply–Demand Risks and Regional Spatial Management in the Yihe River Basin, Central China. *Land* **2021**, *10*, 843. [CrossRef]
4. Hou, P.; Wang, Q.; Shen, W.M.; Zhai, J.; Liu, H.M.; Yang, M. Progress of integrated ecosystem assessment: Concept, framework and challenges. *Geogr. Res.* **2015**, *34*, 1809–1823.
5. Shi, Y.; Shi, D.; Zhou, L.; Fang, R. Identification of ecosystem services supply and demand areas and simulation of ecosystem service flows in Shanghai. *Ecol. Indic.* **2020**, *115*, 106418. [CrossRef]
6. Serna-Chavez, H.M.; Schulp, C.J.E.; Van Bodegom, P.M.; Bouten, W.; Verburg, P.H.; Davidson, M.D. A quantitative framework for assessing spatial flows of ecosystem services. *Ecol. Indic.* **2014**, *39*, 24–33. [CrossRef]
7. Stürck, J.; Poortinga, A.; Verburg, P.H. Mapping ecosystem services: The supply and demand of flood regulation services in Europe. *Ecol. Indic.* **2014**, *38*, 198–211. [CrossRef]
8. Wu, W.; Tang, H.; Yang, P.; You, L.; Zhou, Q.; Chen, Z.; Shibasaki, R. Scenario-based assessment of future food security. *J. Geogr. Sci.* **2011**, *21*, 3–17. [CrossRef]
9. Boithias, L.; Acuña, V.; Vergoñós, L.; Ziv, G.; Marcé, R.; Sabater, S. Assessment of the water supply: Demand ratios in a Mediterranean basin under different global change scenarios and mitigation alternatives. *Sci. Total Environ.* **2014**, *470*, 567–577. [CrossRef]
10. Villa, F.; Bagstad, K.J.; Voigt, B.; Johnson, G.W.; Portela, R.; Honzák, M.; Batker, D. A methodology for adaptable and robust ecosystem services assessment. *PLoS ONE* **2014**, *9*, e91001. [CrossRef]
11. Ma, L.; Liu, H.; Peng, J.; Wu, J. A review of ecosystem services supply and demand. *Acta Geogr. Sin.* **2017**, *72*, 1277–1289.
12. Wu, J.; Fan, X.; Li, K.; Wu, Y. Assessment of ecosystem service flow and optimization of spatial pattern of supply and demand matching in Pearl River Delta, China. *Ecol. Indic.* **2023**, *153*, 110452. [CrossRef]
13. Xia, P.; Peng, J.; Xu, Z.; Gu, T.; Wang, J. Conceptual connotation and quantification methods of ecosystem service flows. *Acta Geogr. Sin.* **2024**, *79*, 584–599.
14. Wang, L.; Zheng, H.; Chen, Y.; Ouyang, Z.; Hu, X. Systematic review of ecosystem services flow measurement: Main concepts, methods, applications and future directions. *Ecosyst. Serv.* **2022**, *58*, 101479. [CrossRef]
15. Zhang, J.; He, C.; Huang, Q.; Li, L. Understanding ecosystem service flows through the metacoupling framework. *Ecol. Indic.* **2023**, *151*, 110303. [CrossRef]
16. Wang, L.; Wu, T.; Zheng, H.; Li, R.; Hu, X.; Ouyang, Z. A comprehensive framework for quantifying ecosystem service flow focusing on social-ecological processes. *Trans. Earth Environ. Sustain.* **2023**, *1*, 20–34. [CrossRef]
17. Du, H.; Zhao, L.; Zhang, P.; Li, J.; Yu, S. Ecological compensation in the Beijing-Tianjin-Hebei region based on ecosystem services flow. *J. Environ. Manag.* **2023**, *331*, 117230. [CrossRef]
18. Jiang, C.; Yang, Z.; Wen, M.; Huang, L.; Liu, H.; Wang, J.; Chen, W.; Zhuang, C. Identifying the spatial disparities and determinants of ecosystem service balance and their implications on land use optimization. *Sci. Total Environ.* **2021**, *793*, 148472. [CrossRef]
19. Koellner, T.; Bonn, A.; Arnhold, S.; Bagstad, K.J.; Fridman, D.; Guerra, C.A.; Kastner, T.; Kissinger, M.; Kleemann, J.; Kuhlicke, C.; et al. Guidance for assessing interregional ecosystem service flows. *Ecol. Indic.* **2019**, *105*, 92–106. [CrossRef]
20. Xiong, X.Y.; Meng, M. Regionalization and optimization strategy of ecological management in Xinjiang, China based on supply-demand relationship and spatial flow of ecosystem services. *J. Appl. Ecol.* **2023**, *34*, 2237–2248.
21. Wu, C.; Lu, R.; Zhang, P.; Dai, E. Multilevel ecological compensation policy design based on ecosystem service flow: A case study of carbon sequestration services in the Qinghai-Tibet Plateau. *Sci. Total Environ.* **2024**, *921*, 171093. [CrossRef]
22. Lin, J.; Huang, J.; Prell, C.; Bryan, B.A. Changes in supply and demand mediate the effects of land-use change on freshwater ecosystem services flows. *Sci. Total Environ.* **2021**, *763*, 143012. [CrossRef]
23. Su, R.; Duan, C.; Chen, B. The shift in the spatiotemporal relationship between supply and demand of ecosystem services and its drivers in China. *J. Environ. Manag.* **2024**, *365*, 121698. [CrossRef]
24. Wang, Q.; Yang, C.H.; Wang, M.L.; Zhao, L.; Zhao, Y.C.; Zhang, Q.P.; Zhang, C.Y. Decoupling analysis to assess the impact of land use patterns on carbon emissions: A case study in the Yellow River Delta efficient eco-economic zone, China. *J. Clean. Prod.* **2023**, *412*, 137415. [CrossRef]
25. Wang, C.; Wang, Y.; Wang, R.; Zheng, P. Modeling and evaluating land-use/land-cover change for urban planning and sustainability: A case study of Dongying city, China. *J. Clean. Prod.* **2018**, *172*, 1529–1534. [CrossRef]
26. Sui, Y.; Sun, D.; Li, S.; Xu, Y.; Wu, J. Study of coastal zone ecosystem restoration in the context of carbon storage change: A case of Dongying City. *Acta Ecol. Sin.* **2021**, *41*, 8112–8123.
27. Jun, Z.; Diandian, J.; Yan, C.; Xin, L.I.U.; Xu, Y.A.N.G.; Peng, H.O.U.; Yanda, X.U. Ecological changes, problems and countermeasures in the High Efficiency Eco-economic Zone of the Yellow River Delta. *Resour. Sci.* **2020**, *42*, 517–526.
28. Jia, Y.; Wang, S.; LIU, F. Land use change and its correlation with habitat quality in high efficiency eco-economic zone of Yellow River Delta. *Bull. Soil Water Conserv.* **2020**, *40*, 213–220.

29. Liu, Y.; Han, M.; Wang, M.; Fan, C.; Zhao, H. Habitat Quality Assessment in the Yellow River Delta Based on Remote Sensing and Scenario Analysis for Land Use/Land Cover. *Sustainability* **2022**, *14*, 15904. [CrossRef]
30. Lu, C.; Cai, X.Q.; Hao, C.S.; Liu, Y.Z.; Wang, Z.Y.; Ma, Y.N. Ecosystem service tradeoff and synergistic relationship in the Yellow River Delta High-Efficiency Eco-Economic Zone. *J. Appl. Ecol.* **2024**, *35*, 457–468.
31. Ya, X.J.; Ren, H.Z.; Dong, X.B.; Zhou, X. Spatio-temporal migration characteristics of wild Chinese Asian elephants based on land use change and ecosystem service supply and demand. *Acta Ecol. Sin.* **2023**, *43*, 1426–1436.
32. Liang, H.Q.; Shen, M.H.; Shao, M.; Yao, P. Construction of carbon sequestration ecological network in Linyi City based on supply and demand of ecosystem service. *J. Appl. Ecol.* **2024**, *35*, 759–768.
33. Hu, Y.; Ming, T.; Chai, C. Research and Analysis on Spatial and Temporal Evolution Pattern of Carbon Emissions Caused by Land Use Change in Shandong Province. *China Transp. Rev.* **2024**, *46*, 167–174.
34. Li, J. Identification of ecosystem services supply and demand and driving factors in Taihu Lake Basin. *Environ. Sci. Pollut. Res.* **2022**, *29*, 29735–29745. [CrossRef] [PubMed]
35. Liu, J.; Wang, J.; Dai, J.; Zhai, T.; Li, Z. The relationship between supply and demand of ecosystem services and its spatio-temporal variation in the Yellow River Basin. *J. Nat. Resour.* **2021**, *36*, 148–161. [CrossRef]
36. Zhao, C.; Xiao, P.; Qian, P.; Xu, J.; Yang, L.; Wu, Y. Spatiotemporal differentiation and balance pattern of ecosystem service supply and demand in the Yangtze River Economic Belt. *Int. J. Environ. Res. Public Health* **2022**, *19*, 7223. [CrossRef]
37. Gao, H.; Fu, T.; Liang, H.; Liu, J. Cold/hot spots identification and tradeoff/synergy analysis of ecosystem services in Taihang Mountain area. *Chin. J. Eco-Agric.* **2022**, *30*, 1045–1053.
38. Yao, C.Y.; An, R.; Dou, C.; Liu, Y.L. Research on construction and evaluation of forest land ecological network in three gorges reservoir area based on MSPA and MCR Model. *Resour. Environ. Yangtze Basin* **2022**, *31*, 1953–1962.
39. Wang, X.; Zhao, P.; Long, Y.X.; Song, W.; Liu, X. Identification of key areas of land space ecological protection and restoration based on the pattern of ecological security in Guangdong, Hong Kong and Macau. *Acta Ecol. Sin.* **2022**, *42*, 450–461.
40. Dong, Z.; Zheng, S.; Zhao, H.; Dong, R. Comparative analysis of methods of wind field simulation based on spatial interpolation. *J. Geo-Inf. Sci* **2015**, *17*, 37–44.
41. Su, D.; Yu, C.A.O.; Dong, X.; Wu, Q.; Fang, X.; Cao, Y. Evaluation of ecosystem services budget based on ecosystem services flow: A case study of Hangzhou Bay area. *Appl. Geogr.* **2024**, *162*, 103150. [CrossRef]
42. Yuan, W.H.; Fan, W.J.; Li, J.C.; Liu, L.M. Research on the Spatiotemporal Differentiation Characteristics and Influencing Factors of Ecological Quality in Typical Counties in the Yellow River Basin. *J. Ecol. Rural Environ.* **2024**, *40*, 622–633.
43. Hasan, S.S.; Zhen, L.; Miah, M.G.; Ahamed, T.; Samie, A. Impact of land use change on ecosystem services: A review. *Environ. Dev.* **2020**, *34*, 100527. [CrossRef]
44. Wang, X.Q.; Zhao, X.Y. Impacts of human activities on ecosystem services in national parks: A case study of Qilian Mountain National Park. *J. Nat. Resour.* **2023**, *38*, 966–982. [CrossRef]
45. Wang, C.; Luo, J.; Tang, H. Analysis on the Driving Force of Spatial and Temporal Differentiation of Carbon Storage in the Taihang Mountains Based on InVEST Model. *Ecol. Environ.* **2023**, *32*, 215. [CrossRef]
46. Lin, Z.Y.; Xiao, Y.; Ouyang, Z.Y. Assessment of ecological importance of the Qinghai-Tibet Plateau based on ecosystem service flows. *J. Mt. Sci.* **2021**, *18*, 1725–1736. [CrossRef]
47. Zhang, X.R.; Wang, X.; Cheng, C.; Liu, S.; Zhou, C. Ecosystem service flows in Karst area of China based on the relationship between supply and demand. *Acta Ecol. Sin.* **2021**, *41*, 3368–3380.

Disclaimer/Publisher's Note: The statements, opinions and data contained in all publications are solely those of the individual author(s) and contributor(s) and not of MDPI and/or the editor(s). MDPI and/or the editor(s) disclaim responsibility for any injury to people or property resulting from any ideas, methods, instructions or products referred to in the content.